



# A model gas study of ammonium formate, methanamide and guanidinium formate as alternative ammonia precursor compounds for the selective catalytic reduction of nitrogen oxides in diesel exhaust gas

Oliver Kröcher<sup>a,\*</sup>, Martin Elsener<sup>a</sup>, Eberhard Jacob<sup>b</sup>

<sup>a</sup> Paul Scherrer Institute, 5232 Villigen PSI, Switzerland

<sup>b</sup> Emissionskonzepte, 82152 Krailling, Germany

## ARTICLE INFO

### Article history:

Received 7 July 2008

Received in revised form 18 September 2008

Accepted 19 September 2008

Available online 9 October 2008

### Keywords:

Selective catalytic reduction

SCR

Urea

Ammonium formate

Methanamide

Guanidine

Guanidinium formate

Decomposition

Hydrolysis

## ABSTRACT

Ammonium formate, methanamide and guanidinium salts were investigated in model gas experiments and found to be suitable ammonia precursor compounds for the selective catalytic reduction (SCR) of nitrogen oxides since they decompose to ammonia over different metal oxide catalysts.

The decomposition of ammonium formate started with thermolysis to formic acid and ammonia. Formic acid reacted further, mainly to water and CO (decarbonylation), but CO<sub>2</sub> formation (decarboxylation) was also observed. Under unsuitable reaction conditions, methanamide may be formed from ammonia and formic acid in an amidation reaction, and HCN may be formed from methanamide by dehydration.

When methanamide was used as a reducing agent, it was emitted undecomposed at temperatures below 250 °C and formed HCN as a side-product at temperatures above 350 °C.

Among the tested guanidinium salts, guanidinium formate best met the requirements for a reducing agent in the SCR process, i.e., it decomposed at moderate temperatures with high selectivity, and it is highly water-soluble and stable when heated to 100 °C.

For guanidinium formate, a similar decomposition mechanism is proposed as that for ammonium formate. First, guanidinium formate thermolyzes to guanidine and formic acid. Then, formic acid is decarbonylated and guanidine is assumed to hydrolyze in three steps, proceeding through urea and isocyanic acid (HNCO) as intermediates to the final product, ammonia.

The formation of side-products was avoided for all three reducing agents when the reactor was filled with TiO<sub>2</sub> (anatase) as a catalyst and operated at 275–350 °C at low space velocities.

© 2008 Elsevier B.V. All rights reserved.

## 1. Introduction

The stepwise reduction of the particle and NO<sub>x</sub> emission limits for commercial vehicles and diesel passenger cars in recent years initiated the development of new engine technologies that resulted in a decrease in NO<sub>x</sub> raw emission levels from approximately 1000 ppm to about 200–300 ppm for the very latest generation of diesel engines. The further reduction in nitrogen oxide emissions in these low-NO<sub>x</sub> engines below the EU VI and US 2010 or EU6 and Tier2 Bin5 limitations, respectively, i.e., to concentrations of about 30 ppm in the exhaust gas, may only be achieved with suitable after-treatment systems. The most efficient process for achieving such low NO<sub>x</sub> concentrations is selective catalytic reduction (SCR) with ammonia, aside from the NO<sub>x</sub> storage and reduction (NSR)

technology [1–3]. The two most important reactions of the SCR process are the NO SCR reaction ( $4\text{NO} + 4\text{NH}_3 + \text{O}_2 \rightarrow 4\text{N}_2 + 6\text{H}_2\text{O}$ ) and the much faster NO/NO<sub>2</sub> SCR reaction ( $2\text{NO} + 2\text{NO}_2 + 4\text{NH}_3 \rightarrow 4\text{N}_2 + 6\text{H}_2\text{O}$ ).

At the early stage of development of the SCR process for mobile applications, the toxic and irritant properties of ammonia, as well as the necessity to use pressure bottles to keep it liquid, were in conflict with its direct utilization in diesel vehicles. Perry and Siebers had the first idea to overcome this problem and suggested the use of cyanuric acid as safe precursor compound for NO<sub>x</sub> reduction in vehicles (the “Raprenox” process) [4]. They postulated in the first instance that isocyanic acid (HNCO) was the actual reducing agent for nitrogen oxides in a homogeneous gas phase reaction. However, reinvestigations revealed that isocyanic acid was only an intermediate, which quickly hydrolyzed to ammonia, and that this ammonia reduced the nitrogen oxides in the SCR reaction on the surface of the steel tube that was used by Perry and Siebers as a reactor in their study. From these results, it was

\* Corresponding author. Tel.: +41 56 310 20 66; fax: +41 56 310 23 23.  
E-mail address: [oliver.kroecher@psi.ch](mailto:oliver.kroecher@psi.ch) (O. Kröcher).

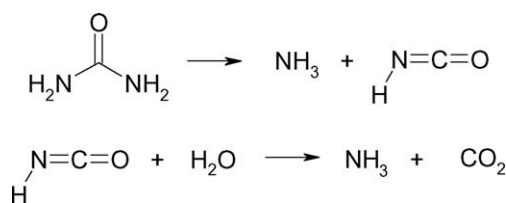


**Fig. 1.** Chemistry of the urea decomposition in the SCR system: thermolysis of urea to ammonia and isocyanic acid and the hydrolysis of isocyanic acid to ammonia and carbon dioxide.

only a small step to the conclusion that urea is a more suitable reducing agent for applications in diesel vehicles, because it readily decomposes to ammonia via isocyanic acid (Fig. 1) and is, therefore, a much better ammonia precursor compound [5,6]. Other facts that support urea as an ammonia precursor compound are its nontoxicity and availability as a bulk commodity produced on a scale of more than 100 million tons per year [7]. The process development was concentrated on aqueous urea solutions due to their advantageous handling properties and resulted finally in the standardization of an eutectic solution of 32.5% urea in water (trade name: AdBlue<sup>®</sup>) as the reducing agent for all SCR systems in diesel vehicles [8]. Despite the advantages of this precursor compound, a number of drawbacks are associated with the application of urea solution, namely its limited storage stability above 50 °C, the tendency to form side-products and deposits in the exhaust gas system, the melting point of −11 °C, requiring expensive heating systems to prevent freezing, and finally the relatively small amount of ammonia (0.2 kg) released from 1 kg of AdBlue<sup>®</sup> [6,9]. The only mobile application of urea SCR so far is in heavy-duty diesel vehicles, for which complex technical measures are acceptable to prevent malfunction of the system. For a short time, SCR systems have been under development for passenger cars [10]. In view of the smaller system dimensions, the lower consumption of the reducing agent and the high cost-sensitivity of this market, complex technical solutions to handle the reducing agent appear unattractive. Instead of that alternative, ammonia precursor compounds with more favorable properties would be desirable. In Table 1, the hitherto investigated ammonia precursor compounds are compared with regard to composition and the

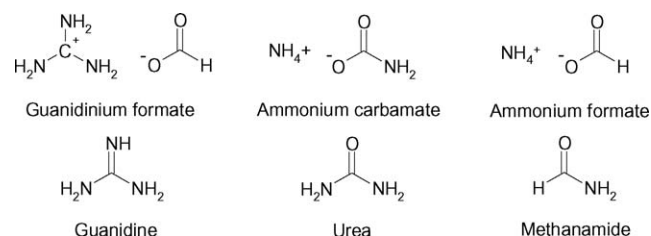


**Fig. 2.** Chemical relationship between different ammonia precursor compounds.

properties most relevant for the SCR process. Solid urea, ammonium carbamate and magnesium hexaammonia chloride elude the freezing problem of urea solution by the utilization of solid compounds instead of liquids in the SCR process. However, regarding the handling and processing problems of solids, a liquid reducing agent is preferred. One possibility to stay with liquids is the addition of a urea solution with the compounds, which significantly lowers the melting point of the mixture without hampering the urea decomposition or the production of harmful emissions. In a first study of Koebel and Elsener in a diesel test rig, it was shown that ammonium formate meets these requirements [19]. In the exhaust gas, ammonium formate first dissociates to ammonia and formic acid, which further decomposes to water and CO at higher temperatures. For a review of known SCR reducing agents and a broader introduction into the topic, please refer to [11,21,22].

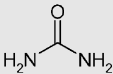
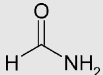
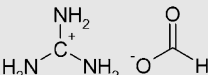
Aside from additives for urea solution, urea might also be completely substituted by other ammonia generating compounds. From considerations of the chemical relationship between urea, ammonium carbamate and ammonium formate in Fig. 2, two other related ammonia precursors can be deduced, which might be interesting as urea substitutes: methanamide and guanidinium formate. An 80% aqueous solution of methanamide meets the physicochemical properties for an applicable liquid reducing agent: (a) stability at 100 °C, (b) a melting point of −28 °C, (c) evaporation without leaving a residue or decomposition and (d) biodegradability. Moreover, this solution has a 50% higher ammonia formation potential than AdBlue<sup>®</sup>. The major drawback of methanamide is its teratogenicity, which might be acceptable

**Table 1**  
Overview of known ammonia precursor compounds [11].

Ammonia precursor compound		m.p. [°C]	b.p. [°C]	Composition [wt.%]					NH <sub>3</sub> content		Ref.
				Ammonia	Urea	AC	AF	H <sub>2</sub> O	[kg/kg]	[kg/L]	
Liquid ammonia	NH <sub>3</sub>	−78	−33	100					1.00	0.61	[12]
Ammonia solution	NH <sub>3</sub> ·xH <sub>2</sub> O			10				90	0.10	0.10	
Urea solution (AdBlue <sup>®</sup> )		−11	Decomposition		32.5			76.5	0.20	0.22	[13]
Solid urea		133	Decomposition		100				0.57	0.42	[14,15]
Ammonium carbamate (AC)		NH <sub>3</sub> release already at RT				100			0.44		[16,17]
Urea + ammonium formate solution (AF, Denoxium)		−26/−30	Decomposition		20		26	54	0.20	0.22	[18,19]
AdAmmine	Mg(NH <sub>3</sub> ) <sub>6</sub> Cl <sub>2</sub>	Stepwise NH <sub>3</sub> release		52					0.52	0.62	[20]

**Table 2**

Comparison of new ammonia precursor compounds with urea.

Ammonia precursor compound		Melting point [°C]	Boiling point [°C]	Composition [wt.%]				NH <sub>3</sub> content	
				Urea	GuFo	Methanamide	H <sub>2</sub> O	[kg/kg]	[kg/L]
Urea solution (AdBlue <sup>®</sup> )		−11	Decomposition	32.5			67.5	0.20	0.22
Methanamide (AdAmide)		−28	210			80	20	0.30	0.33
Guanidinium formate (GuFo)		≈−30 <sup>a</sup>	≈100 <sup>a</sup>		60		40	0.29	0.32

<sup>a</sup> Preliminary results from Nigu Chemie GmbH.

concerning the very similar effect of gasoline [21]. The second proposed ammonia precursor is guanidine, which is in fact not applicable in its free form, but may be stabilized by different harmlessly decomposable anions such as formate, oxalate or carbonate [23]. Preliminary investigations indicated that a 60% solution of guanidinium formate is the most promising for SCR applications [11], exhibiting a very low melting point and almost the same high ammonia formation potential as an 80% methanamide solution. Moreover, it proved to be very stable when heated for several months to a temperature of 60 °C [24]. The main advantage of guanidinium formate compared to methanamide is its probable nontoxicity in analogy to the non-toxic classification of guanidinium thiocyanate, carbonate, and nitrate [25]. Table 2 summarizes the properties of the proposed new ammonia precursor solutions with a 32.5% urea solution (AdBlue<sup>®</sup>) as reference. The low water content in both formulations is favorable, since thermodynamic calculations for the urea solution showed that the heat of evaporation for water is dominating the overall energy demand for the production of gaseous ammonia from aqueous solutions of reducing agents [26]. It should not go unnoticed that the new ammonia precursors are certainly more expensive than urea and that their application is only economically justifiable in view of their advantageous properties, notably their low melting points, which allows to design SCR systems without expensive electric heating.

In the present study, the decomposition properties of ammonium formate, methanamide and guanidinium formate were investigated in laboratory and pilot plant experiments with respect to their application as SCR reducing agents. In a recent technical paper, we mainly gave an introduction into the topic and reviewed the hitherto known ammonia precursor compounds along with a few selected results of our laboratory investigations [11].

## 2. Experimental

Fe-ZSM5 (0.90 g,  $S_{\text{BET}} = 250 \text{ m}^2/\text{g}$ ) and  $\text{V}_2\text{O}_5/\text{WO}_3\text{-TiO}_2$  (1.23 g,  $S_{\text{BET}} = 50\text{--}60 \text{ m}^2/\text{g}$ ) catalysts prepared at PSI were coated on cordierite monoliths (400 cpsi,  $9 \times 13$  cells,  $L = 39 \text{ mm}$ ,  $V = 7.7 \text{ cm}^3$ ) according to [27,28]. The catalytic converters were tested with different reducing agents in a temperature controlled quartz reactor at a GHSV of  $52\,000 \text{ h}^{-1}$  with nitrogen as the base feed containing 10% oxygen and 5% water [29]. The  $\text{NO}_x$  reduction efficiency was measured with variable amounts of reducing agents and 1000 ppm NO or 500 ppm NO + 500 ppm  $\text{NO}_2$  in the feed, respectively. All gases were dosed by electronic mass flow controllers and water by a liquid flow controller via a downstream evaporator.

Either the feed or the product gas could be sucked with a constant temperature of 180 °C at a flow of 150  $\text{L}_\text{N}/\text{h}$  through a gas measuring cell with a volume of 200 mL and 2 m pathlength, built in a HR-FTIR spectrometer, model “Nexus”, from Thermo Electron. This setup, in combination with a multi-component method for the correction of non-linear responses and cross-sensitivities, facilitated the quantification of the possible gas components NO,  $\text{NO}_2$ ,  $\text{N}_2\text{O}$ ,  $\text{NH}_3$ ,  $\text{H}_2\text{O}$ , CO,  $\text{CO}_2$ , isocyanic acid (HNCO), nitric acid ( $\text{HNO}_3$ ), formic acid ( $\text{HCOOH}$ ), formaldehyde ( $\text{H}_2\text{CO}$ ), methanamide ( $\text{HCONH}_2$ ) and hydrocyanic acid (HCN) with an accuracy of  $\pm 1\%$  and a detection limit of 1 ppm.

For the sake of simplicity, the dosage of ammonium formate solution was substituted by ammonia and formic acid feeds in the laboratory. Ammonia was dosed from a gas bottle containing 5%  $\text{NH}_3$  in  $\text{N}_2$  and formic acid was transferred into the gas phase by saturation of a nitrogen flow in two consecutive wash bottles filled with formic acid. The concentrations of both components were adjusted by electronic mass flow controllers such that equimolar amounts of ammonia and formic acid were dosed in the range of 0–1200 ppm each. Prior to the experiments, the blank conversion of formic acid was measured without catalyst. Below 450 °C the formic acid conversion was negligible and even at 500 °C, only 13% conversion was measured. The main product was  $\text{CO}_2$ , with a selectivity of more than 70% along with CO. The dosage of ammonia plus formic acid gave the same result.

Methanamide was dosed in the decomposition and SCR experiments by temperature-controlled evaporation of 16.1 g/h of a 4.77% aqueous solution of methanamide (puriss. p.a., >99.5%, Fluka) into a mixture of oxygen and nitrogen at a rate of  $0.40 \text{ m}^3_\text{N}/\text{h}$  to yield a gas feed of 1000 ppm methanamide, 10%  $\text{O}_2$  and 5%  $\text{H}_2\text{O}$  in  $\text{N}_2$ .

The guanidine derivatives used in this study were provided by AlzChem Trostberg GmbH and Nigu Chemie GmbH. Guanidinium oxalate and carbonate could be prepared as solids, but the formate is very hygroscopic and was hence produced as 40% and 60% aqueous solutions.

Guanidinium hydrogen carbonate was prepared in a 100 mL gas-washing bottle equipped with a frit by bubbling a gas flow of 14%  $\text{CO}_2$  in  $\text{N}_2$  ( $25.7 \text{ L}_\text{N}/\text{h}$ ) through 70 g of a 15% aqueous di-guanidinium carbonate solution until a constant pH value of 8.4 was reached. The course of the pH value during the introduction of  $\text{CO}_2$  was recorded with a universal titrator from Metrohm, type 809 Titrando.

The generation of a uniform spray pattern with small droplets and a narrow cone angle is a prerequisite for realistic model gas investigations with liquid reducing agents. Since this is very difficult on a laboratory scale, SCR measurements with guanidi-

nium salt solutions gave only unreliable results, which cannot be directly used for an upscale of the process. Therefore, we abstained from our first attempt to measure realistic  $\text{NO}_x$  reduction efficiencies with guanidinium derivatives on a laboratory scale and, instead of that, investigated only their decomposition properties relative to a urea solution as a reference sample. This allowed us to order the decomposition properties of the different guanidinium salts and to identify the best suited ammonia precursor for SCR. Moreover, this simple approach was sufficient to screen potential materials for the catalytic decomposition of guanidinium derivatives.

For the preliminary laboratory tests of the decomposition properties of guanidinium salt solutions, the following setup was used: the guanidinium salt solutions were dosed dropwise through an eccentrically moved thin Teflon capillary (<0.2 mm) from the top of an upright heated quartz reactor with an inner diameter of 28 mm onto the entrance area of the monolith catalysts. The distance from the capillary to the catalyst surface was 25 cm and the model gas in the reactor was composed of 10%  $\text{O}_2$  and 5%  $\text{H}_2\text{O}$  in  $\text{N}_2$  at a flow rate of  $0.45 \text{ m}_\text{N}^3/\text{h}$ . The reducing agents were injected such that the deposition of droplets at the reactor walls was avoided. At a dosing rate of 3.5 g/h this resulted in 0.25–0.33 droplets/s with an average size of 3–4  $\mu\text{L}$ , which were evenly distributed over an area of about  $1 \text{ cm}^2$ . The catalyst bed was composed of 3 or 5 discs of coated cordierite monoliths (400 cpsi, diameter = 26 mm, height = 12 mm), which were installed out of phase in order to maximize the probability of capturing the reducing agent droplets.

Fe-ZSM5 (details see above),  $\text{TiO}_2$  (DT51 Millenium Chemicals; loading 125 g/L),  $\gamma\text{-Al}_2\text{O}_3$ ,  $\text{ZrO}_2$ , and  $\text{TiO}_2$  doped with lanthanum oxide (DT57 von Millenium Chemicals) were tested as catalytic coatings for the guanidine derivative decomposition. The concentrations of the reducing agent solutions were chosen such that at a fixed dosing rate of 3.5 g/h, a  $\text{NH}_3$  concentration of 900–1000 ppm was reached in the model gas flow for total hydrolysis. This condition was met for 18% guanidinium formate, 15% guanidinium carbonate, 19.5% guanidinium hydrogen carbonate and 15% urea (reference) in water, respectively.

The pilot plant experiments were performed in the test apparatus depicted in Fig. 3 [30]. A maximum  $300 \text{ m}_\text{N}^3/\text{h}$  of air was dosed by an electronic mass flow controller (Bronkhorst, type F-206), humidified with  $5 \text{ m}_\text{N}^3/\text{h}$  of steam and heated in two parallel electrical air heaters (1). The two air flows were merged after the heaters and the gas stream relaxed in the tube (2), before 10–800 g/h of reducing agent was injected through a gas-

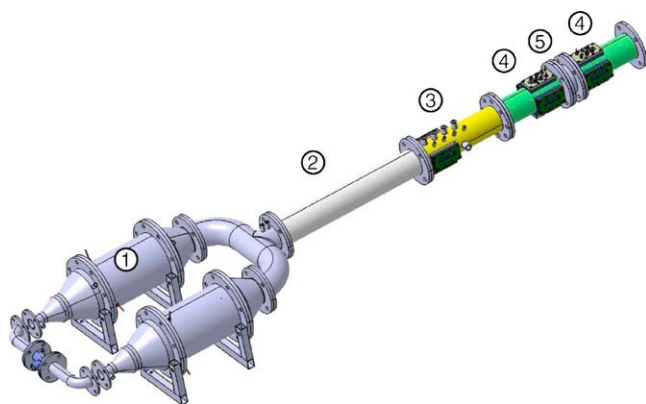


**Fig. 3.** Pilot plant for the test of hydrolysis catalysts (H-Cats) from [30]. (1) Two gas heaters in parallel. (2) Flow relaxation. (3) Injection of reducing agent. (4) Windows or sensor flanges for thermocouples, pressure transducers, and sampling for FTIR spectroscopy. (5) Catalyst mounting.

atomizing nozzle (3). Windows, thermocouples, pressure transducers and sampling tubes for FTIR spectroscopy, which were installed up- and downstream of the catalysts at position (4), allowed for the inspection and analysis of the decomposition processes. The following three catalysts were mounted in series at position (5): (a) Metal substrate from Emitec, type 40 MXPE with corrugated channels, coated with  $\text{TiO}_2$ , diameter = 100 mm, length = 110 mm,  $V = 0.86 \text{ L}$ . (b) Metal substrate from Emitec, smooth channels, 200 cpsi, coated with  $\text{TiO}_2$ , diameter = 100 mm, length = 110 mm,  $V = 0.86 \text{ L}$ . (c) Bed of ca. 1.5 kg  $\text{TiO}_2$  pellets (pellet diameter = 6 mm, length = 10–25 mm), diameter = 100 mm, length = 220 mm,  $V = 1.73 \text{ L}$ . For details about the structures of the metal substrates, refer to [21]. The gas phase was analyzed by IR spectroscopy with an FTIR spectrometer from Thermo Electron, type NEXUS 470, which was equipped with a heated 2 m multipath gas cell. The raw spectra were evaluated at the Paul Scherrer Institute with the multi-component method described above. Since this method was developed on another instrument of the same type, the accuracy of the analysis results was somewhat reduced to ca.  $\pm 3\%$ .

### 3. Results and discussion

#### 3.1. Ammonium formate as SCR reducing agent

##### 3.1.1. NO SCR with ammonium formate over $\text{V}_2\text{O}_5/\text{WO}_3\text{-TiO}_2$

Ammonium formate was tested as an SCR reducing agent by dosing formic acid and ammonia in equimolar amounts, which is an acceptable simplification since ammonium formate partly dissociates in the gas phase. The equilibrium of this reaction is

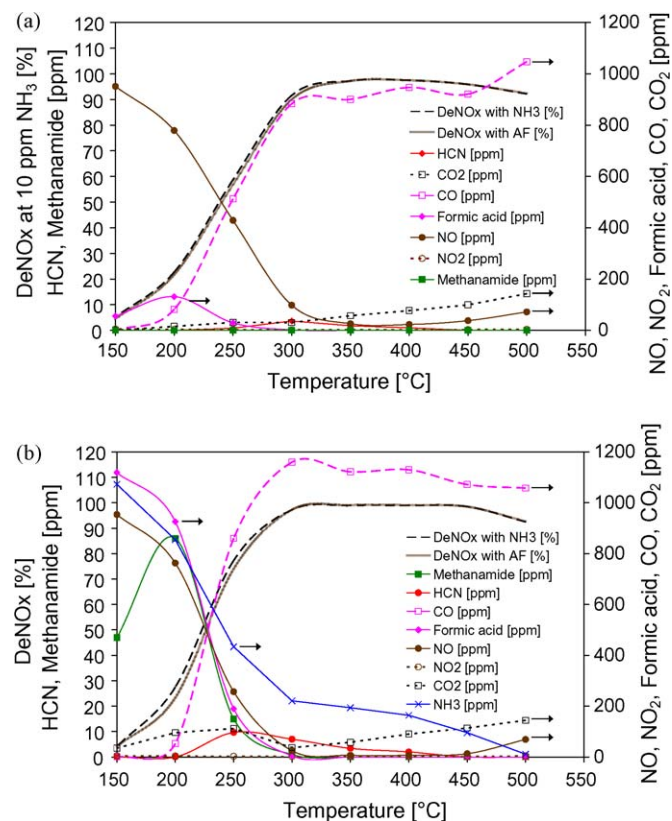


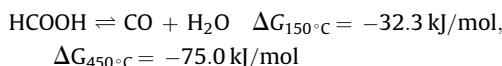
**Fig. 4.** NO SCR performance with ammonia + formic acid over  $\text{V}_2\text{O}_5/\text{WO}_3\text{-TiO}_2$ . (a)  $\text{DeNO}_x$  at optimal dosage of ammonia + formic acid, i.e., at 10 ppm ammonia slip. (b)  $\text{DeNO}_x$  at  $\alpha = (\text{ammonia} + \text{formic acid})_{\text{in}}/\text{NO}_{x,\text{in}} = 1.2$ . Feed: 10%  $\text{O}_2$ , 5%  $\text{H}_2\text{O}$ , 1000 ppm NO, 0–1200 ppm  $\text{NH}_3$  + formic acid (1:1) in  $\text{N}_2$ . GHSV =  $52\,000 \text{ h}^{-1}$ .



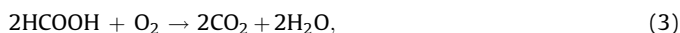
shifted to the products ammonia and formic acid when the temperature is increased:



In Fig. 4a, the NO SCR performance over  $\text{V}_2\text{O}_5/\text{WO}_3\text{-TiO}_2$  is compared for  $\text{NH}_3$  and ammonia + formic acid as reducing agents. The measuring unit  $\text{DeNO}_x$  at 10 ppm ammonia slip refers to practice-oriented conditions in which the amount of reducing agent is controlled such that a 10 ppm ammonia slip was always observed. Compared to  $\text{NH}_3$  as the reducing agent, the NO SCR performance over  $\text{V}_2\text{O}_5/\text{WO}_3\text{-TiO}_2$  was only slightly affected by the presence of formic acid. The main decomposition product of formic acid found was CO, which was almost quantitatively formed above 300 °C according to:



Other than CO, small amounts of  $\text{CO}_2$  were found, which may be formed by the direct oxidation of formic acid with oxygen

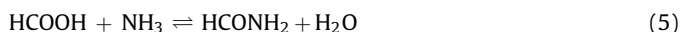


the decomposition of formic acid to  $\text{CO}_2$  and  $\text{H}_2$ ,



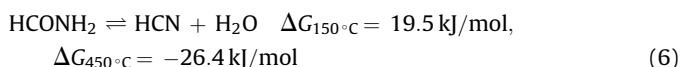
or the decomposition of formic acid to CO and water with subsequent oxidation of CO at elevated temperatures. At  $T < 300$  °C, increasing emissions of formic acid were observed, with 30 ppm at 250 °C and 130 ppm at 200 °C. At 150 °C, the formic acid emissions decrease again, but only due to the much lower dosing rate of ammonia + formic acid at this temperature. When calculating the formic acid emissions relative to the amount of ammonia + formic acid dosed, the part of unconverted formic acid increases steadily with decreasing temperatures. HCN was observed in traces between 250 and 350 °C.

The picture changed somewhat in an experiment with  $\alpha = \text{NH}_{3,\text{in}}/\text{NO}_{x,\text{in}} = 1.2$ , which simulated potential overdosing situations for the reducing agent during vehicle operation. In this case (Fig. 4b), very high concentrations of formic acid were observed at low temperatures as expected, but also high methanamide ( $\text{HCONH}_2$ ) emissions between 150 and 250 °C, which were not observed at the optimum dosage of the reducing agent. As amides in general are easily formed from carbonic acids and amines at elevated temperatures, the production of methanamide is not surprising under these conditions, where formic acid and ammonia are present in excess:



The methanamide concentration increases from 150 to 200 °C in accordance with the initiation of amide formation. However, at somewhat higher temperatures, the light-off temperature of the SCR reaction is reached, thereby consuming ammonia, which is no longer available for the side-reaction to form methanamide. As a consequence, the methanamide concentration drops in opposition to the increase of the SCR activity.

Another difference, observable for overdosing of the reducing agent, was the significantly increased concentration of HCN at intermediate temperatures, which may be formed by the dehydration of methanamide in a typical consecutive reaction:



This reaction sequence is in accordance with the appearance of maximum HCN formation after the maximum of methanamide

formation. Moreover, the dehydration of methanamide to HCN is endergonic at low temperatures (150 °C), which is in agreement with the absence of HCN at these conditions, although the parent compound methanamide is already present in considerable concentrations. In contrast, high temperatures favor the formation of HCN from methanamide as the free enthalpy of the reaction is becoming negative ( $\Delta G_{450^\circ\text{C}} = -26.4 \text{ kJ/mol}$ ). The HCN concentration, however, declines after an intermediate maximum due to a lack of the reactant methanamide at higher temperatures. At medium temperatures with free enthalpies around zero, the equilibrium of the reaction may be influenced most easily. With water in excess, the equilibrium should be shifted towards methanamide and the generation of HCN should be suppressed.

It is worthwhile to have a look at the  $\text{CO}_2$  emissions also, which significantly increased at low temperatures, with a maximum at 250 °C, when ammonia + formic acid was overdosed. Considering the above-mentioned possible pathways to  $\text{CO}_2$  in the reaction mixture, additional experiments were carried out in order to establish the actual route to  $\text{CO}_2$  at both low and high temperatures. The formation of  $\text{CO}_2$  by the oxidation of CO at elevated temperatures could be ruled out by dosing 1000 ppm CO, 10%  $\text{O}_2$  and 5%  $\text{H}_2\text{O}$  over a vanadia-based SCR catalyst, showing only negligible amounts of  $\text{CO}_2$ : only 16 ppm were formed at 550 °C and much less at lower temperatures (figure not shown). In order to differentiate between the direct decomposition of formic acid to  $\text{CO}_2$  (Reaction (4)) and the formation of  $\text{CO}_2$  by the oxidation of formic acid (Reaction (3)) or methanamide by the oxygen in the feed gas, formic acid and ammonia + formic acid were dosed over  $\text{V}_2\text{O}_5/\text{WO}_3\text{-TiO}_2$  without oxygen in the feed. For formic acid only, almost the same amounts of  $\text{CO}_2$  were found (Fig. 5a) as for formic acid and oxygen (figure not shown), proving that formic acid in fact

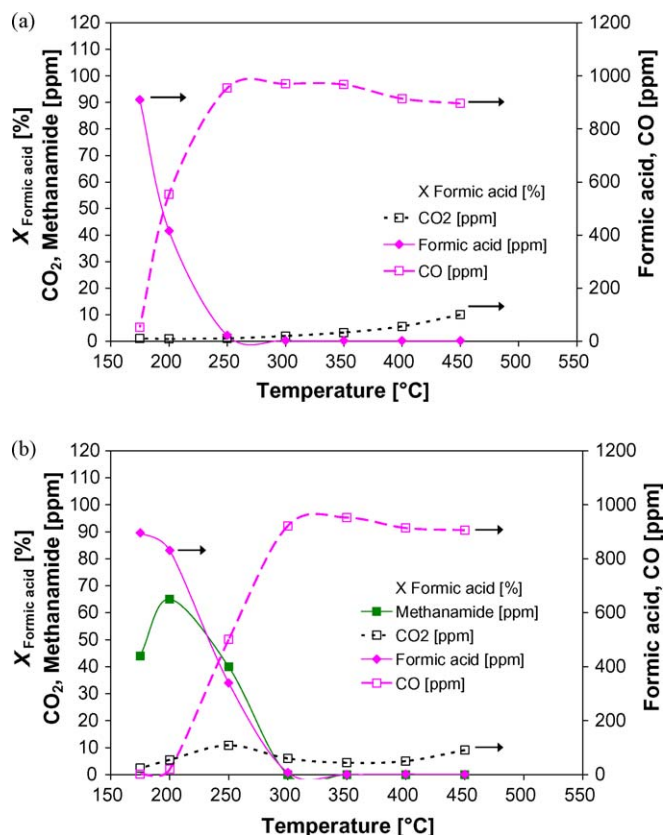


Fig. 5. Reaction of formic acid over  $\text{V}_2\text{O}_5/\text{WO}_3\text{-TiO}_2$  without oxygen. (a) 1000 ppm formic acid. (b) 1000 ppm formic acid + 1000 ppm  $\text{NH}_3$ . Basis feed: 5%  $\text{H}_2\text{O}$  in  $\text{N}_2$ . GHSV = 52 000  $\text{h}^{-1}$ .

partly decomposes to  $\text{CO}_2$  over SCR catalysts beside the standard decomposition pathway to CO. Moreover, the concentration profiles of  $\text{CO}_2$  in these experiments were also almost the same as under NO SCR conditions at optimum ammonia dosage (Fig. 4a), ruling out the contribution of any direct oxidation process to the formation of  $\text{CO}_2$  in this more complex reaction mixture.

Regarding only elevated temperatures, it is remarkable that, in general, almost equal  $\text{CO}_2$  concentration profiles were found in all experiments irrespective of the other reactants beside formic acid, i.e., oxygen, ammonia, NO or  $\text{NO}_2$ . However, at low temperatures, the  $\text{CO}_2$  production varied significantly. For instance, without ammonia or  $\text{NO}_x$  in the feed, almost constant  $\text{CO}_2$  concentrations were found when reducing the temperature from 300 to 150 °C (Fig. 5a). But this  $\text{CO}_2$  production significantly increased at low temperatures, with a maximum at 250 °C, when 1000 ppm  $\text{NH}_3$  was added to the feed (Fig. 5b). When the formic acid conversions are compared, the lower decomposition rate is obvious in the presence of  $\text{NH}_3$  at low temperatures. These observations may be explained by a stabilization of formic acid by ammonia as formate anion at low temperatures. The shift from formic acid to formate favors the decarboxylation (4) relative to the decarbonylation (2), whereby a mechanistic explanation requires a detailed analysis of the transitions states as shown for the example in [31].

### 3.1.2. NO/ $\text{NO}_2$ SCR with ammonium formate over $\text{V}_2\text{O}_5/\text{WO}_3\text{-TiO}_2$

Regarding the NO/ $\text{NO}_2$  SCR reaction over  $\text{V}_2\text{O}_5/\text{WO}_3\text{-TiO}_2$ , formic acid has only a small influence on the  $\text{NO}_x$  reduction efficiency (Fig. 6a). The course of the formic acid decomposition is

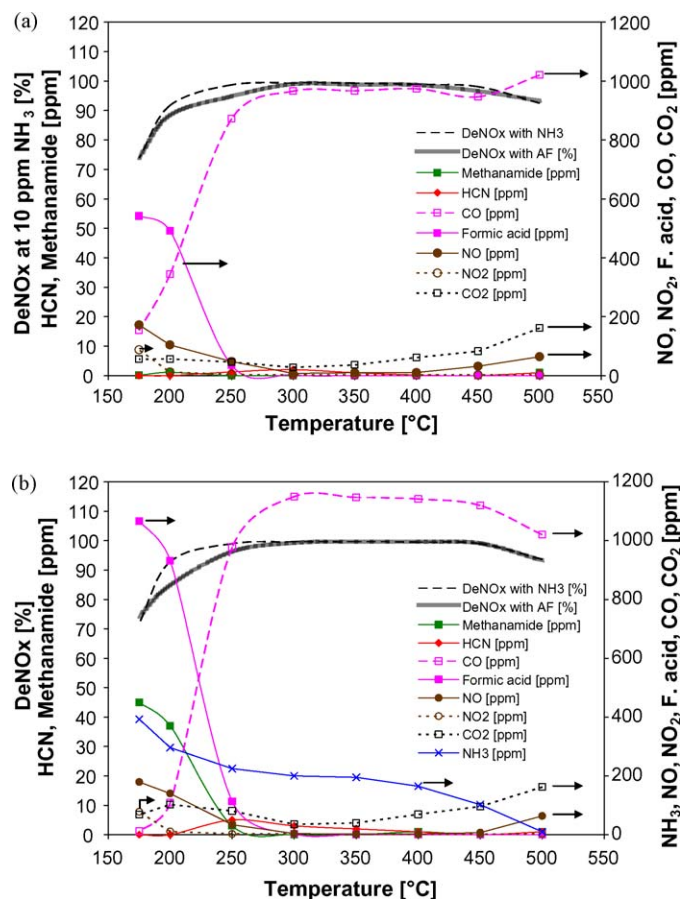
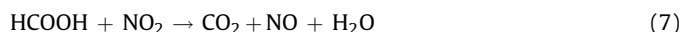


**Fig. 6.** NO/ $\text{NO}_2$  SCR with ammonia + formic acid over  $\text{V}_2\text{O}_5/\text{WO}_3\text{-TiO}_2$ . (a) DeNO<sub>x</sub> at 10 ppm ammonia slip. (b) DeNO<sub>x</sub> at  $\alpha = 1.2$ . Feed: 10%  $\text{O}_2$ , 5%  $\text{H}_2\text{O}$ , 500 ppm NO, 500 ppm  $\text{NO}_2$ , 0–1200 ppm  $\text{NH}_3$  + formic acid (1:1) in  $\text{N}_2$ , GHSV = 52 000  $\text{h}^{-1}$ .

similar to the behavior during NO SCR. Above 300 °C, mainly CO is formed and clearly less  $\text{CO}_2$ . At 250 °C, the formic acid emission was 35 ppm at 10 ppm ammonia slip, which is comparable to NO SCR. However, at 200 °C the formic acid concentration increased up to 500 ppm after the catalyst. This increase compared to the NO SCR experiment is due to the already very high  $\text{NO}_x$  conversion with NO/ $\text{NO}_2$  mixtures at 200 °C and the associated higher dosing rates of ammonia + formic acid to reach the 10 ppm ammonia slip downstream of the SCR catalyst. Also for NO/ $\text{NO}_2$  SCR, HCN was found in traces and noteworthy amounts of methanamide were observed at 175 and 200 °C when the reducing agent was overdosed, i.e.,  $\alpha = \text{NH}_{3,\text{in}}/\text{NO}_{x,\text{in}} = 1.2$ , and resulted in an ammonia slip of 300–400 ppm at this temperature (Fig. 6b). Notably, the  $\text{NO}_x$  reduction efficiency at low temperatures was clearly lower with ammonia + formic acid than with ammonia alone, irrespective of the amount of reducing agent dosed (Fig. 6a and b). The reason for this behavior seemed to be correlated with the preferred consumption of  $\text{NO}_2$  compared to NO, which is typical for reaction systems containing oxidizable hydrocarbons [32]. Following this argumentation,  $\text{NO}_2$  oxidized formic acid to  $\text{CO}_2$  and was thereby itself reduced to NO, which is less SCR active than  $\text{NO}_2$ .



This reaction was verified in a separate experiment in which formic acid was dosed over  $\text{V}_2\text{O}_5/\text{WO}_3\text{-TiO}_2$  along with 500 ppm NO and 500 ppm  $\text{NO}_2$  (Fig. 7). The addition of NO and  $\text{NO}_2$  promoted the total formic acid conversion due to the consumption of ammonia, which stabilizes formic acid. Less CO was produced by the direct decomposition of formic acid to CO and water, but more  $\text{CO}_2$  was found compared to the same experiments without NO and  $\text{NO}_2$  (figure not shown) and without NO,  $\text{NO}_2$  and  $\text{O}_2$  (Fig. 5a). From the course of the NO,  $\text{NO}_2$  and  $\text{CO}_2$  concentration in Fig. 7, it is evident that  $\text{NO}_2$  indeed reacted with formic acid to form  $\text{CO}_2$  and NO. For instance, at 150 °C, 300 ppm  $\text{NO}_2$  and 700 ppm NO were emitted along with 200 ppm  $\text{CO}_2$ , i.e., from the original 500 ppm  $\text{NO}_2$ , 200 ppm had been consumed in the oxidation of 200 ppm formic acid to 200 ppm  $\text{CO}_2$ . The 200 ppm  $\text{NO}_2$  were thereby converted to 200 ppm NO, which added to the original 500 ppm NO dosed.

### 3.1.3. NO SCR with ammonium formate over Fe-ZSM5

Similar to  $\text{V}_2\text{O}_5/\text{WO}_3\text{-TiO}_2$ , NO SCR over Fe-ZSM5 was only weakly influenced by formic acid above 350 °C. However, the already low  $\text{NO}_x$  reduction efficiency over Fe-ZSM5 below 350 °C was further reduced in the presence of formic acid (Fig. 8a). This decrease was even more pronounced when the reducing agent was

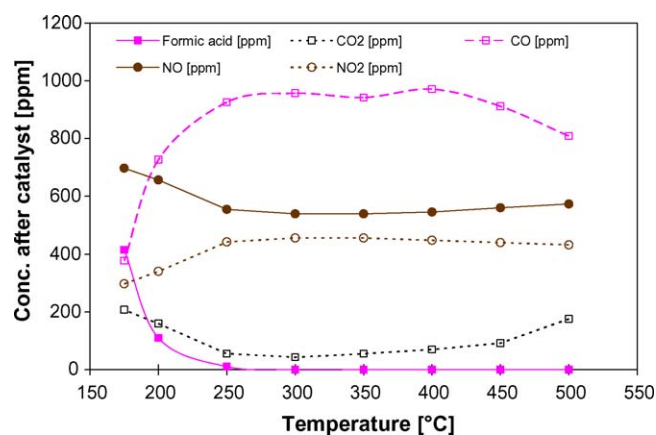


**Fig. 7.** Reaction of formic acid over  $\text{V}_2\text{O}_5/\text{WO}_3\text{-TiO}_2$  in the presence of NO and  $\text{NO}_2$ . Feed: 10%  $\text{O}_2$ , 5%  $\text{H}_2\text{O}$ , 1000 ppm formic acid, 500 ppm NO, 500 ppm  $\text{NO}_2$  in  $\text{N}_2$ , GHSV = 52 000  $\text{h}^{-1}$ .

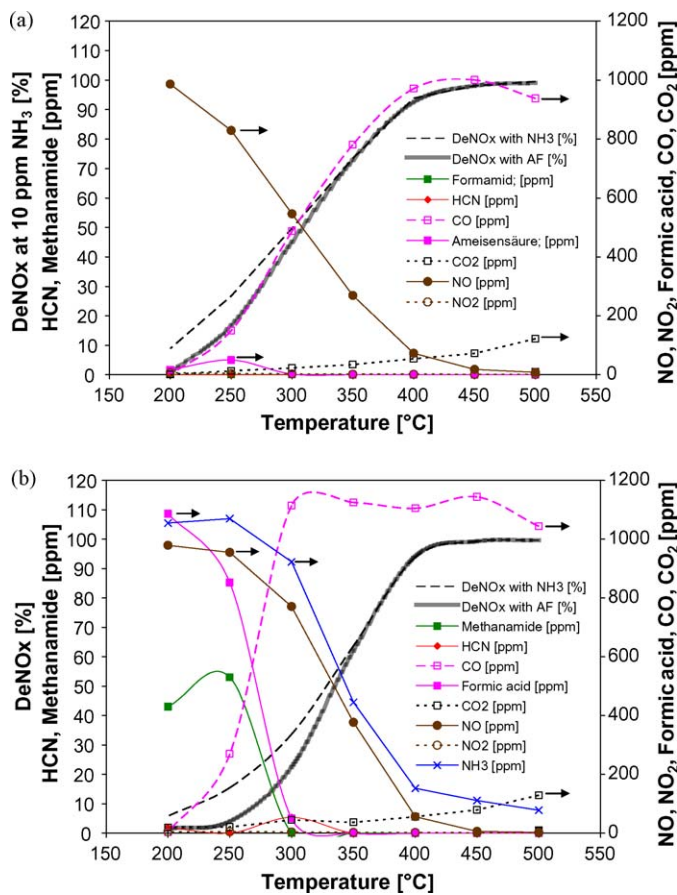


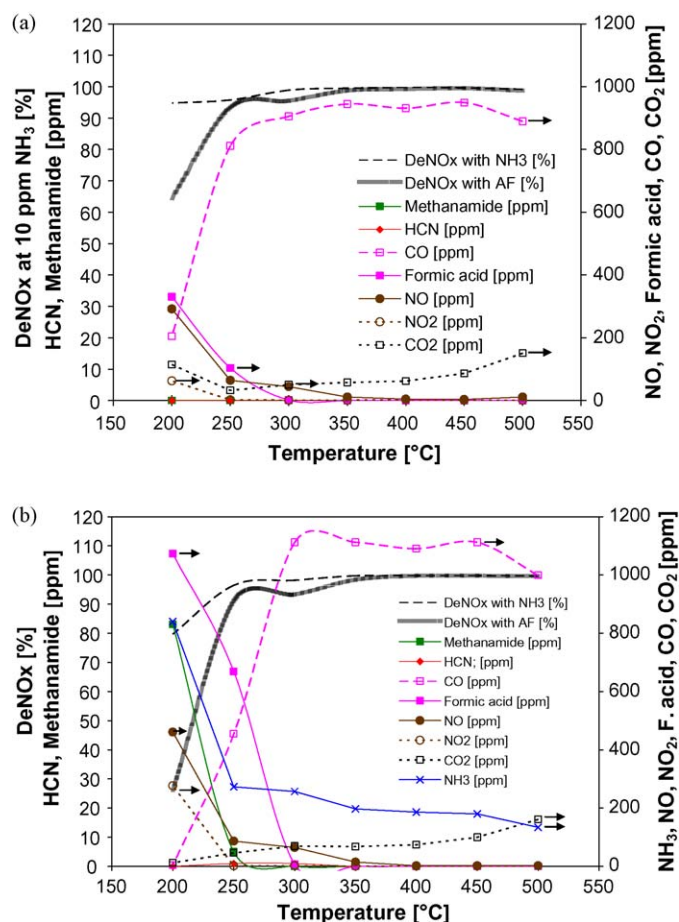
**Fig. 8.** NO SCR with ammonia + formic acid over Fe-ZSM5. (a) DeNO<sub>x</sub> at optimal dosage of ammonia + formic acid, i.e., at 10 ppm ammonia slip. (b) DeNO<sub>x</sub> at  $\alpha = 1.2$ . Feed: 10% O<sub>2</sub>, 5% H<sub>2</sub>O, 1000 ppm NO, 0–1200 ppm NH<sub>3</sub> + formic acid (1:1) in N<sub>2</sub>. GHSV = 52 000 h<sup>-1</sup>.

overdosed (Fig. 8b). This difference in the NO SCR performance is probably caused by the small pores of the zeolites, in which ammonia and formic acid are stabilized as ammonium formate at low temperatures.

Compared to V<sub>2</sub>O<sub>5</sub>/WO<sub>3</sub>-TiO<sub>2</sub>, less methanamide and HCN was formed at  $\alpha = 1.2$  over Fe-ZSM5. Another difference of V<sub>2</sub>O<sub>5</sub>/WO<sub>3</sub>-TiO<sub>2</sub> is the production of methanamide up to 300 °C and a parallel shift of the maximum of the HCN production from 250 to 300 °C. This result is in line with the about 50 °C higher *T*<sub>50</sub> temperature (temperature at 50% conversion) of the NO SCR reaction over Fe-ZSM5 compared to V<sub>2</sub>O<sub>5</sub>/WO<sub>3</sub>-TiO<sub>2</sub>. The slower start of the SCR reaction resulted in higher ammonia concentrations, which may form methanamide with formic acid, followed by the consecutive dehydration of methanamide to HCN. Another interesting feature is that there is no maximum in CO<sub>2</sub> formation over Fe-ZSM5 at low temperatures. It seems that Fe-ZSM5 does not catalyze formic acid decomposition in contrast to V<sub>2</sub>O<sub>5</sub>/WO<sub>3</sub>-TiO<sub>2</sub>.

### 3.1.4. NO/NO<sub>2</sub> SCR with ammonium formate over Fe-ZSM5

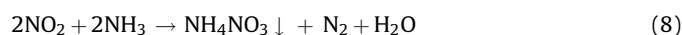
Also for NO/NO<sub>2</sub> SCR over Fe-ZSM5, DeNO<sub>x</sub> was hardly affected above 300 °C, but decreased significantly at lower temperatures (Fig. 9a). At optimum dosage, i.e., at 10 ppm ammonia slip, the NO<sub>x</sub> reduction efficiencies were reduced by 1/3 compared to pure ammonia as the reducing agent. At  $\alpha = 1.2$ , DeNO<sub>x</sub> decreased even by 2/3 (Fig. 9b). The reduced NO<sub>x</sub> reduction efficiency is caused by the oxidation of formic acid by NO<sub>2</sub>. The part of the NO<sub>2</sub> that was consumed in the oxidation of formic acid and converted to NO was missing for the NO/NO<sub>2</sub> SCR reaction and reacted instead in the



**Fig. 9.** NO/NO<sub>2</sub> SCR with ammonia + formic acid over Fe-ZSM5. (a) DeNO<sub>x</sub> at 10 ppm ammonia slip. (b) DeNO<sub>x</sub> at  $\alpha = 1.2$ . Feed: 10% O<sub>2</sub>, 5% H<sub>2</sub>O, 500 ppm NO, 500 ppm NO<sub>2</sub>, 0–1200 ppm NH<sub>3</sub> + formic acid (1:1) in N<sub>2</sub>. GHSV = 52 000 h<sup>-1</sup>.

much slower NO SCR reaction. With rising temperatures, the NO/NO<sub>2</sub> SCR reaction rate increased much faster than the rate of oxidation of formic acid by NO<sub>2</sub>, such that this reaction did not play a role above 300 °C. When NO/NO<sub>2</sub> SCR over V<sub>2</sub>O<sub>5</sub>/WO<sub>3</sub>-TiO<sub>2</sub> (Fig. 6a) is compared with Fe-ZSM5 (Fig. 9a), the stronger deactivation of the Fe-ZSM5 catalyst is obvious.

This deactivation of Fe-ZSM5 at low temperatures is even more severe for overdosage than for the optimum dosage of ammonia + formic acid along with much higher formic acid and huge methanamide emissions at 200 °C (Fig. 9b). It is remarkable that almost 277 ppm NO<sub>2</sub> and almost 461 ppm NO, but no CO<sub>2</sub>, are emitted at 200 °C, which means that the NO/NO<sub>2</sub> SCR reactivity was not lowered at the expense of the reaction of NO<sub>2</sub> with formic acid to form CO<sub>2</sub> and NO. There must be another deactivation mechanism. The nitrogen balance revealed a NH<sub>3,react</sub>/NO<sub>x,react</sub> ratio of 1.06 after subtraction of the amount of ammonia reacting to methanamide. Only (500–461) ppm = 39 ppm NO and 39 ppm NO<sub>2</sub> reacted with (2 · 39) ppm = 78 ppm NH<sub>3</sub> to nitrogen in the NO/NO<sub>2</sub> SCR reaction. The residual (277–39) ppm = 238 ppm NO<sub>2</sub> reacted with ammonia in another reaction with 1:1 stoichiometry. Since beside NO and NO<sub>2</sub>, only traces of N<sub>2</sub>O (3 ppm, not shown in Fig. 9b) and no other nitrogen containing compounds were found in the product gas stream, the only conclusion left is that NO<sub>2</sub> reacted with NH<sub>3</sub> to ammonium nitrate and nitrogen, which is the only reaction of NO<sub>2</sub> and NH<sub>3</sub> with a 1:1 stoichiometry, in line with the observed NH<sub>3,react</sub>/NO<sub>x,react</sub> ratio of 1.06:





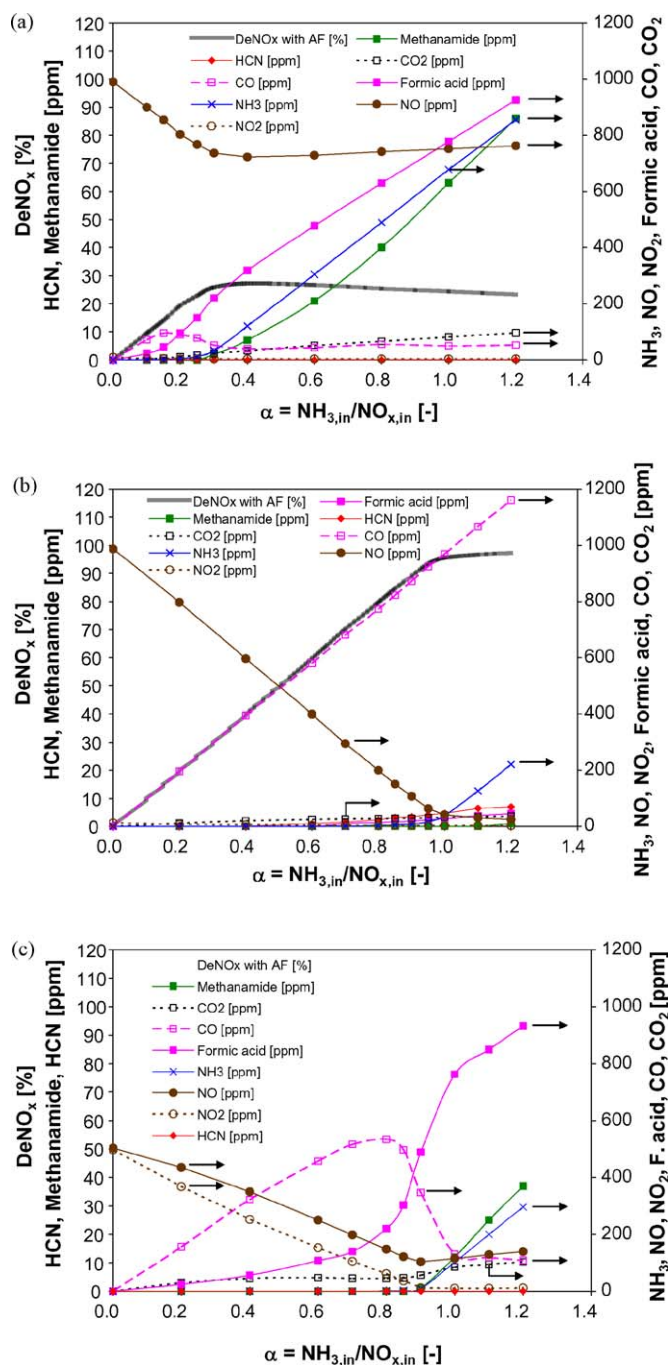


**Fig. 10.** SCR with ammonia + formic acid over  $V_2O_5/WO_3-TiO_2$ . (a) NO SCR with 1000 ppm NO at 200 °C. (b) NO SCR with 1000 ppm NO at 300 °C. (c) NO/ $NO_2$  SCR with 500 ppm NO and 500 ppm  $NO_2$  at 200 °C. Feed: 10%  $O_2$ , 5%  $H_2O$ , 0–1200 ppm  $NH_3$  + formic acid (1:1) in  $N_2$ . GHSV = 52 000  $h^{-1}$ .

The possible  $NO_2$  SCR reaction ( $3NO_2 + 4NH_3 \rightarrow 3.5N_2 + 6H_2O$ ) can be ruled out since in this reaction, 1.33 moles of  $NH_3$  are consumed for every mole of  $NO_2$  reduced. The absence of the typical decomposition products of ammonium nitrate  $HNO_3$  ( $NH_4NO_3 \leftrightarrow HNO_3 + NH_3$ ) and  $N_2O$  ( $NH_4NO_3 \rightarrow N_2O + 2H_2O$ ) in the product gas indicates that ammonium nitrate was deposited on the catalyst at 200 °C. This behavior of Fe-ZSM5 differs from vanadia-based catalysts, for which ammonium nitrate deposition was not observed above 180 °C. In [32], the thermodynamic stability of ammonium nitrate was plotted versus the concentration of  $HNO_3$  and  $NH_3$ . It is obvious that in the small pores of the

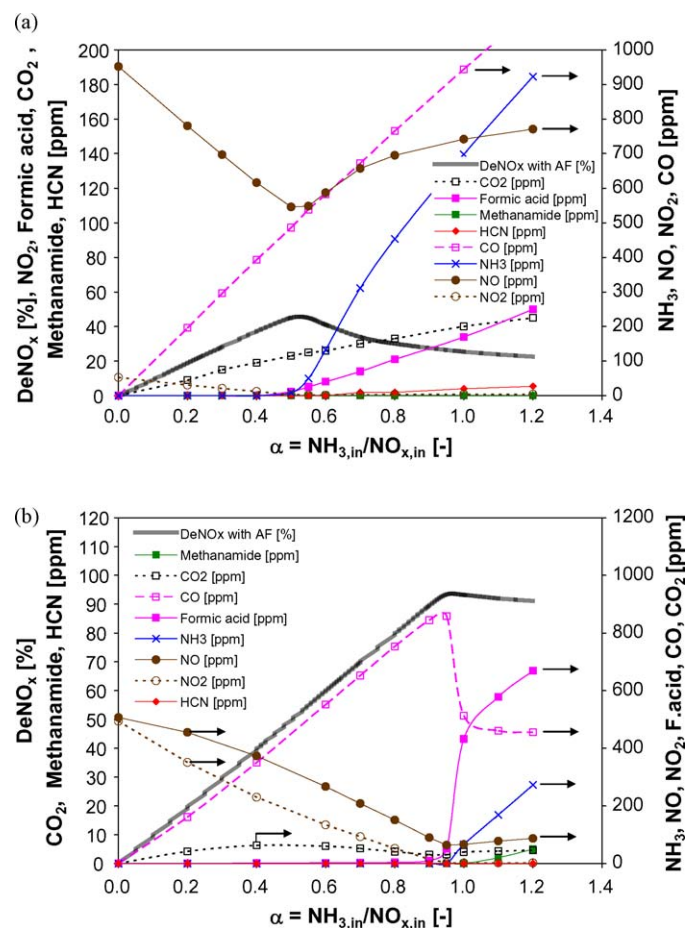


**Fig. 11.** SCR with ammonia + formic acid over Fe-ZSM5. (a) NO SCR with 1000 ppm NO at 300 °C. (b)  $NO/NO_2$  SCR with 500 ppm NO and 500 ppm  $NO_2$  at 250 °C. Feed: 10%  $O_2$ , 5%  $H_2O$ , 0–1200 ppm  $NH_3$  + formic acid (1:1) in  $N_2$ . GHSV = 52 000  $h^{-1}$ .

zeolite, high local concentrations of  $HNO_3$  and  $NH_3$  are present, resulting in a stabilization of ammonium nitrate in the liquid form.

### 3.1.5. Features of SCR with ammonium formate

In another representation of the experimental data, more details become apparent about the behavior of ammonium formate during SCR over  $V_2O_5/WO_3-TiO_2$  and Fe-ZSM5. In Figs. 10 and 11, the emissions of all components are plotted versus the dosing ratio  $\alpha = NH_{3,in}/NO_{x,in}$ .  $V_2O_5/WO_3-TiO_2$  shows the expected behavior when ammonia + formic acid is dosed under NO SCR conditions at 200 and 300 °C (Fig. 10a and b). With increasing  $NH_3$  dosage, first a linear increase of the  $NO_x$  reduction efficiency (De $NO_x$ ) is observed, which approaches a low plateau at 200 °C (Fig. 10a) and almost total conversion at 300 °C (Fig. 10b), in accordance with the steeply increasing catalyst activities at low temperatures. When the amount of reducing agent is further increased, ammonia emissions start to increase. At 200 °C, the  $NO_x$  reduction efficiency decreases again for overdosage of the reducing agent, due to a typical inhibiting effect of  $NH_3$  on SCR over vanadia-based catalysts [33]. CO runs through a maximum, followed by an increase of the formic acid emissions. The relationship of CO, formic acid, ammonia and methanamide emissions over  $V_2O_5/WO_3-TiO_2$  can be identified much better during NO/ $NO_2$  SCR at 200 °C (Fig. 10c). The most prominent feature in the concentration curves of the different components is that CO and formic acid emissions show an inverse course. As long as less ammonia was dosed than was being consumed in the SCR reaction, i.e., ammonia



reacted completely, formic acid decomposed to CO. On the other hand, formic acid was stabilized by excess ammonia as ammonium formate at higher dosing ratios, resulting in a drop of the CO emissions and a steep increase of formic acid, ammonia and methanamide emissions, the latter being formed in an amidation reaction from ammonia and formic acid.

From Fig. 11a, showing the NO SCR reaction over Fe-ZSM5 in dependency of the dosing ratio at 300 °C, a much stronger decrease of the NO<sub>x</sub> reduction efficiency is discernible for overdosage of the reducing agent than over V<sub>2</sub>O<sub>5</sub>/WO<sub>3</sub>-TiO<sub>2</sub>. This behavior is in line with the described pronounced inhibiting by ammonia on the SCR reaction over Fe-ZSM5 [34]. Another interesting detail is the production of 53 ppm NO<sub>2</sub> from NO without dosage of ammonia + formic acid, which is in contrast to the behavior of the vanadia-based catalyst, but in line with the high catalytic activity of the Fe<sup>2+</sup>/Fe<sup>3+</sup> redox couple for the reaction  $\text{NO} + 0.5\text{O}_2 \leftrightarrow \text{NO}_2$  [34]. The stabilizing effect of ammonia on formic acid was even more pronounced during NO/NO<sub>2</sub> SCR over Fe-ZSM5 at 250 °C, which is shown in Fig. 11b, where formic acid is quantitatively converted to CO in ammonia deficient conditions. However, once ammonia was present in excess, the CO concentration dropped and formic acid emissions increased in a step-like fashion.

This stabilizing effect of ammonia on formic acid was investigated in separate experiments over V<sub>2</sub>O<sub>5</sub>/WO<sub>3</sub>-TiO<sub>2</sub> and Fe-ZSM5 at different temperatures. Formic acid was not stabilized by ammonia at 300 °C on both catalysts (results not shown). At 250 °C, formic acid was totally converted to CO over both catalysts without ammonia dosage (Fig. 12a and b). However, when ammonia was

dosed it had a stabilizing effect on formic acid over the vanadia-based SCR catalyst and a very strong effect over Fe-ZSM5. Only 50 ppm of ammonia was sufficient to reduce the conversion of 1000 ppm formic acid from 100% to 53%, i.e., 470 ppm formic acid was stabilized (Fig. 12b). With increasing ammonia dosage, the formic acid conversion was further reduced. However, the conversion ran through a minimum and increased again slightly for higher ammonia concentrations due to increased methanamide formation. The course of the CO<sub>2</sub> concentration is remarkable: it mirrors the curve shape of the formic acid conversion, which suggests a relationship between unconverted formic acid and CO<sub>2</sub> formation. At 200 °C, the formic acid conversion was further reduced and the CO<sub>2</sub> formation was much more pronounced (results not shown).

There are two possible explanations for this stabilizing effect of ammonia on formic acid. Either the small amounts of ammonia covered the Brønsted acid sites of Fe-ZSM5, which catalyze the formic acid decomposition, or ammonium formate was stably deposited in the very small pores of the zeolite during the equilibration time of the experiment. As a consequence, the ammonium formate in the pores blocked the active sites for formic acid decomposition. Since the vanadia-based catalysts are also very acidic and adsorb ammonia very strongly, but did not show such a pronounced deactivation for formic acid decomposition, the deposition of ammonium formate in the pores seems to be the more probable explanation.

In order to check this hypothesis, Temperature Programmed Desorption (TPD) experiments were performed with both catalysts. First, the NO/NO<sub>2</sub> SCR reaction was carried out with 500 ppm NO, 500 ppm NO<sub>2</sub> and 1000 ppm NH<sub>3</sub> + formic acid (1:1) at 200 °C. Then, the NO<sub>x</sub>, NH<sub>3</sub> and formic acid dosage was stopped and the weakly adsorbed species were isothermally desorbed at 200 °C. The strongly adsorbed components were also desorbed in the following heating phase up to 500 °C.

After stopping the NO/NO<sub>2</sub> SCR reaction over V<sub>2</sub>O<sub>5</sub>/WO<sub>3</sub>-TiO<sub>2</sub>, weakly adsorbed formic acid beside small amounts of the reaction products CO, CO<sub>2</sub> and methanamide desorbed completely within a very short time, whereas ammonia was much more tailing over a period of 15 min due to its much stronger adsorption (Fig. 13a). Only ammonia was released in the final heating phase.

The Fe-ZSM5 catalyst desorbed much more ammonia and formic acid compared to the V<sub>2</sub>O<sub>5</sub>/WO<sub>3</sub>-TiO<sub>2</sub> catalyst in the isothermal phase of the TPD experiment (Fig. 13b; Table 3). Almost all formic acid could be desorbed by purging with nitrogen at constant temperature within the first 20 min. The nearly congruent desorption pattern of formic acid and ammonia is suggestive of the adsorption of these components in the form of ammonium formate on the catalyst surface. The ammonia and formic acid, released in huge amounts at the beginning of purging, immediately form methanamide. Moreover, formic acid partly decomposed to CO<sub>2</sub> and CO. During the heating phase, about 150 ppm CO and HCN desorbed along with large amounts of ammonia and traces of CO<sub>2</sub> and formic acid. HCN was formed from ammonium formate and methanamide in the heating phase. In the final isothermal heating phase at 500 °C almost congruent desorption patterns of ammonia and HNO<sub>3</sub> are noticeable, which seem to be desorbed in equimolar amounts taking into account the superposed tailing of the major ammonia desorption peak (Table 3). This observation is a clear indication of the formation of ammonium nitrate on Fe-ZSM5. The apparent high decomposition temperatures for ammonium nitrate indicate that this compound was deposited not only on the catalyst, but also in the tubes downstream of the catalyst, where much lower temperatures were applied, resulting in only slow desorption. The observed deactivation of the catalyst in the catalytic tests is not

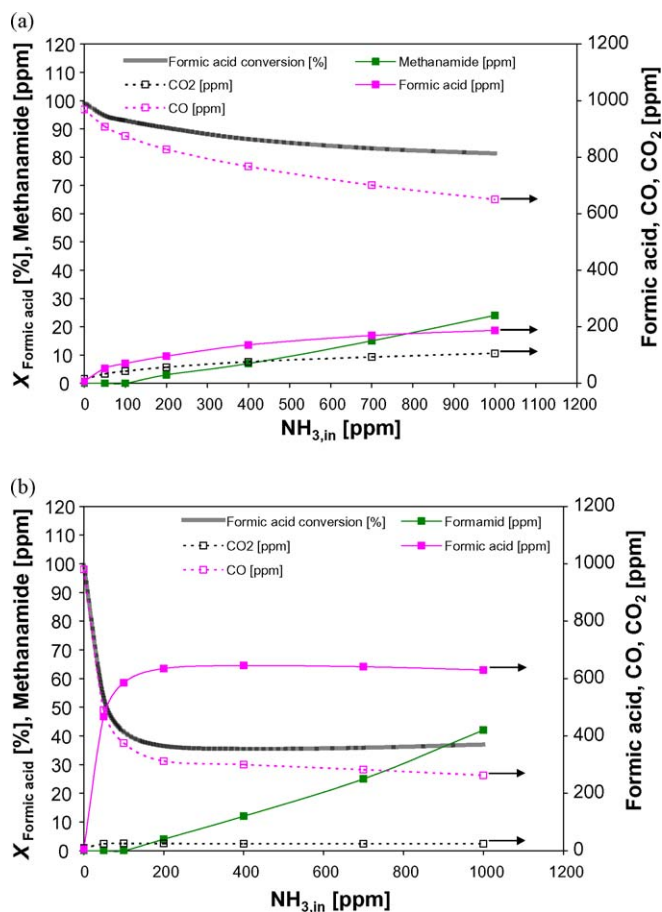


Fig. 12. Influence of NH<sub>3</sub> on the formic acid decomposition over (a) V<sub>2</sub>O<sub>5</sub>/WO<sub>3</sub>-TiO<sub>2</sub> and (b) Fe-ZSM5. Feed: 10% O<sub>2</sub>, 5% H<sub>2</sub>O, 1000 ppm formic acid, 0–1000 ppm NH<sub>3</sub> in N<sub>2</sub>. T = 250 °C. GHSV = 52 000 h<sup>-1</sup>.

**Table 3**

Amounts of desorbed compounds in the different phases of the temperature programmed desorption after NO/NO<sub>2</sub> SCR with ammonia + formic acid ( $\alpha = 1.0$ ,  $T = 200^\circ\text{C}$ ) over V<sub>2</sub>O<sub>5</sub>/WO<sub>3</sub>-TiO<sub>2</sub> and Fe-ZSM5. GHSV = 52 000 h<sup>-1</sup>.

	NH <sub>3</sub> [ $\mu\text{mol/g}_{\text{Cat.}}$ ]	Formic acid [ $\mu\text{mol/g}_{\text{Cat.}}$ ]	CO [ $\mu\text{mol/g}_{\text{Cat.}}$ ]	CO <sub>2</sub> [ $\mu\text{mol/g}_{\text{Cat.}}$ ]	HCN [ $\mu\text{mol/g}_{\text{Cat.}}$ ]	Methanamide [ $\mu\text{mol/g}_{\text{Cat.}}$ ]	HNO <sub>3</sub> [ $\mu\text{mol/g}_{\text{Cat.}}$ ]
V <sub>2</sub> O <sub>5</sub> /WO <sub>3</sub> -TiO <sub>2</sub>							
$T = 200^\circ\text{C}$	65	55	8	1	0	1	2
Heating 200 $\rightarrow$ 500 $^\circ\text{C}$	39	1	1	0	0	0	1
$T = 500^\circ\text{C}$	7	1	0	0	0	0	0
Sum	111	57	9	1	0	1	3
Fe-ZSM5							
$T = 200^\circ\text{C}$	317	236	14	20	0	22	28
Heating 200 $\rightarrow$ 500 $^\circ\text{C}$	233	9	33	11	24	0	7
$T = 500^\circ\text{C}$	175	3	1	10	0	0	121
Sum	725	248	48	40	24	22	156

surprising in view of the huge amounts of compounds adsorbed and stored on the catalyst surface (725  $\mu\text{mol/g}_{\text{Cat.}}$ , Table 3).

### 3.2. Methanamide as SCR reducing agent

Independent from the experiments with ammonium formate, in which methanamide was formed as side-product, methanamide itself was suggested as an ammonia precursor compound in the SCR process. Methanamide may be converted with water to ammonia and formic acid in the backward reaction of (5):



Calculations of the free enthalpy showed that the reaction of equimolar amounts of methanamide and water is slightly

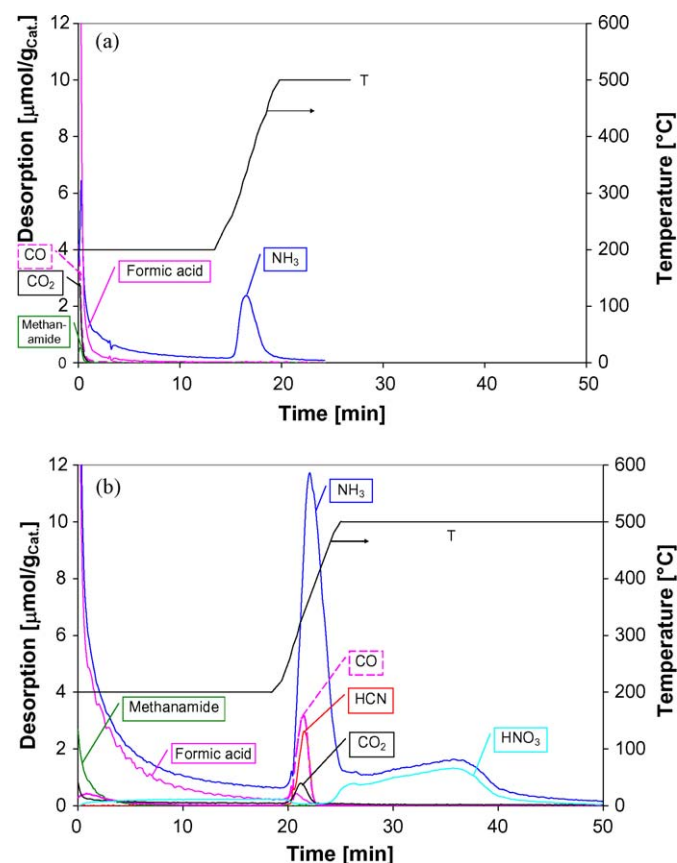


**Fig. 13.** Temperature programmed desorption after NO/NO<sub>2</sub> SCR with ammonia + formic acid ( $\alpha = 1.0$ ,  $T = 200^\circ\text{C}$ ) over (a) V<sub>2</sub>O<sub>5</sub>/WO<sub>3</sub>-TiO<sub>2</sub> and (b) Fe-ZSM5. GHSV = 52 000 h<sup>-1</sup>.

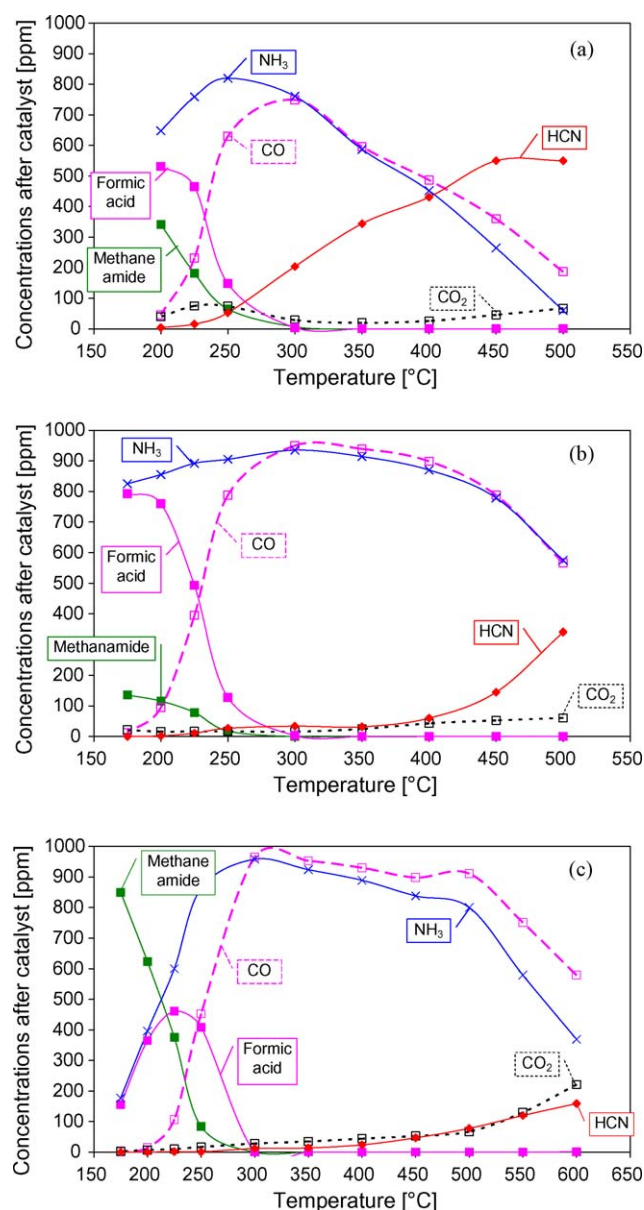


**Fig. 14.** Decomposition of methanamide over (a) V<sub>2</sub>O<sub>5</sub>/WO<sub>3</sub>-TiO<sub>2</sub>, (b) TiO<sub>2</sub> and (c) Fe-ZSM5. Feed: 10% O<sub>2</sub>, 5% H<sub>2</sub>O, 1000 ppm methanamide in N<sub>2</sub>. GHSV = 52 000 h<sup>-1</sup>.

endergonic at 150 °C, with  $\Delta G = 2.175$  kJ/mol. But the reaction does not become exergonic until 450 °C, which means that the equilibrium is shifted to the product side. Due to the only slightly positive value for the free enthalpy below 450 °C, the thermodynamic equilibrium can be influenced by the concentration of the reactants. Applying realistic concentrations for methanamide (1000 ppm) and water (5%) in the thermodynamic calculations resulted in only 10 ppm unreacted methanamide at 100 °C. For higher temperatures, the equilibrium is completely on the side of the products ammonia and formic acid.

First, we tried to hydrolyze methanamide over a  $V_2O_5/WO_3$ - $TiO_2$  catalyst at a space velocity of  $52\,000\text{ h}^{-1}$ , which is equivalent to the conditions for an injection into the main exhaust flow of an SCR system (Fig. 14a). It turned out that methanamide was not completely converted below 250 °C, and that formic acid emissions were additionally observed. For temperatures above 250 °C, methanamide and formic acid were indeed no longer detected, but larger amounts of HCN were found instead.

In this respect,  $TiO_2$  proved to be much more suitable. High methanamide conversions to ammonia and CO were observed at 200 °C, and HCN was formed in appreciable amounts only above 400 °C (Fig. 14b). Methanamide also decomposed very easy to ammonia and CO over Fe-ZSM5 (Fig. 14c). Similar to  $TiO_2$ , the temperature window between 300 and 400 °C may be used for the quantitative ammonia production. The additional dosage of NO (NO SCR) involved no further improvement of the methanamide decomposition over both  $V_2O_5/WO_3$ - $TiO_2$  and Fe-ZSM5 (figures not shown). However, the addition of NO plus  $NO_2$  (NO/ $NO_2$  SCR) resulted in a significant reduction of the methanamide emissions at low temperatures over both catalysts (Fig. 15a and b).

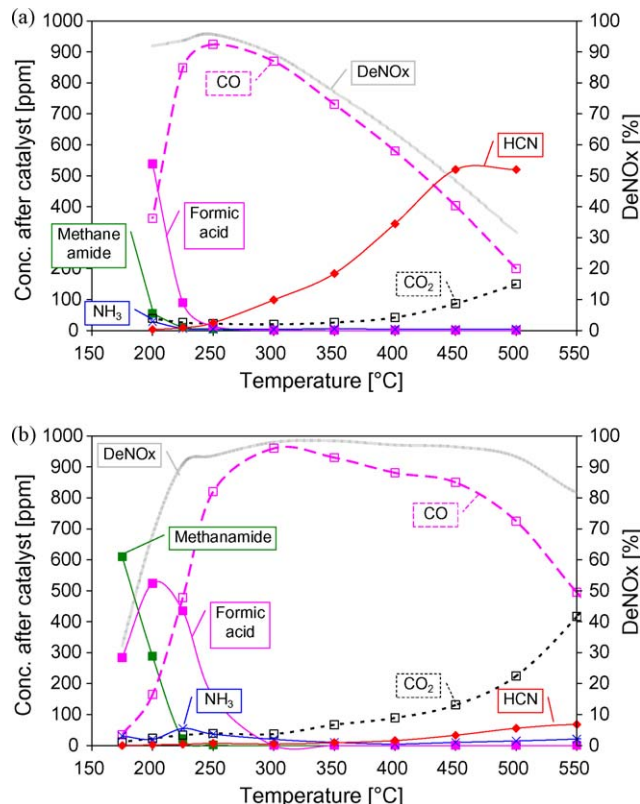


Fig. 15. NO/ $NO_2$  SCR with methanamide over (a)  $V_2O_5/WO_3$ - $TiO_2$  and (b) Fe-ZSM5. DeNO<sub>x</sub> at 10 ppm ammonia slip. Feed: 10%  $O_2$ , 5%  $H_2O$ , 500 ppm NO, 500 ppm  $NO_2$ , 0–1200 ppm methanamide in  $N_2$ . GHSV =  $52\,000\text{ h}^{-1}$ .

Table 4

Thermohydrolysis of guanidinium salts over different catalysts coated on cordierite monoliths (400 cpsi). Dosage of the reducing agent by dropping the reducing agent on the catalyst entrance. GHSV =  $13\,000\text{ h}^{-1}$ . Basis feed gas: 5%  $H_2O$  in  $N_2$ .

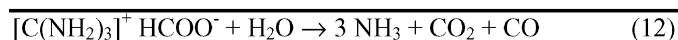
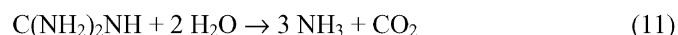
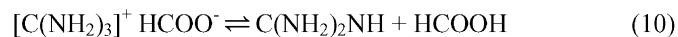
$T_{cat}$ [°C]	Ammonia precursor compound	Catalyst	$O_2$ [%]	$Y_{CO_2}$ [%]	$Y_{NH_3}$ [%]	HNCO [ppm]	CO [ppm]	HCOOH [ppm]	Methanamide [ppm]	HCN [ppm]
300	Urea solution (15%)	Fe-ZSM5	10	100	92	<1	<1	<1	<1	<1
300	Urea solution (15%)	Fe-ZSM5	0	100	97	<1	<1	<1	<1	<1
350	Urea solution (15%)	Fe-ZSM5	0	100	98	<1	<1	<1	<1	<1
300	Guanidinium formate solution (18%)	Fe-ZSM5	10	22	25	<1	130	35	<1	<1
350	Guanidinium formate solution (18%)	Fe-ZSM5	10	78	67	2	185	47	5	17
350	Guanidinium formate solution (18%)	Fe-ZSM5	0	67	68	3	200	61	7	15
400	Guanidinium formate solution (18%)	Fe-ZSM5	0	96	93	2	276	7	<1	25
450	Guanidinium formate solution (18%)	Fe-ZSM5	10	126	71	4	220	7	<1	12
450	Guanidinium formate solution (18%)	Fe-ZSM5	0	102	96	4	280	10	<1	16
250	Urea solution (15%)	$TiO_2$	10	102	96	<1	<1	<1	<1	<1
300	Urea solution (15%)	$TiO_2$	10	103	99	<1	<1	<1	<1	<1
250	Guanidinium formate solution (18%)	$TiO_2$	10	85	73	<1	177	67	6	10
300	Guanidinium formate solution (18%)	$TiO_2$	10	104	90	<1	250	<1	<1	9
350	Guanidinium formate solution (18%)	$TiO_2$	10	111	96	<1	286	1	<1	6
250	di-Guanidinium oxalate solution (18%)	$TiO_2$	10	13	14	<1	13	1	<1	<1
300	di-Guanidinium oxalate solution (18%)	$TiO_2$	10	52	50	1	90	1	<1	7
350	di-Guanidinium oxalate solution (18%)	$TiO_2$	10	79	76	1	144	<1	<1	16
250	Guanidinium formate solution (18%)	$\gamma$ - $Al_2O_3$	10	6	6	1	5	30	<1	<1
300	Guanidinium formate solution (18%)	$\gamma$ - $Al_2O_3$	10	34	37	2	89	100	12	1
350	Guanidinium formate solution (18%)	$\gamma$ - $Al_2O_3$	10	67	64	2	230	7	2	11
400	Guanidinium formate solution (18%)	$\gamma$ - $Al_2O_3$	10	109	95	2	309	5	<1	30
350	di-Guanidinium oxalate solution (18%)	$\gamma$ - $Al_2O_3$	10	71	66	2	96	2	<1	28
400	di-Guanidinium oxalate solution (18%)	$\gamma$ - $Al_2O_3$	10	84	80	3	134	2	<1	20
250	Guanidinium formate solution (18%)	$La_2O_3/TiO_2$	10	42	46	<1	83	88	9	3
300	Guanidinium formate solution (18%)	$La_2O_3/TiO_2$	10	95	94	<1	305	11	2	30
350	Guanidinium formate solution (18%)	$La_2O_3/TiO_2$	10	97	93	<1	320	<1	<1	7
250	di-Guanidinium oxalate solution (18%)	$La_2O_3/TiO_2$	10	8	13	<1	8	2	<1	1
300	di-Guanidinium oxalate solution (18%)	$La_2O_3/TiO_2$	10	55	57	<1	90	1	<1	9
350	di-Guanidinium oxalate solution (18%)	$La_2O_3/TiO_2$	10	70	70	<1	128	1	<1	4
400	di-Guanidinium oxalate solution (18%)	$La_2O_3/TiO_2$	10	83	83	<1	154	<1	<1	7
350	Guanidinium formate solution (18%)	$ZrO_2$	10	41	49	21	95	128	22	3
400	Guanidinium formate solution (18%)	$ZrO_2$	10	52	57	29	130	127	19	14



### 3.3. Guanidinium derivatives as SCR reducing agents

#### 3.3.1. Preliminary tests in the laboratory

Guanidinium formate should be catalytically decomposable in a two-step reaction under ammonia formation. Due to the high stability of guanidinium formate, its direct hydrolysis in analogy to reaction (9) is difficult. A quantitative conversion should nevertheless be possible if a dissociation equilibrium of guanidinium formate with guanidine ( $\text{C}(\text{NH}_2)_2\text{NH}$ ) and formic acid is presumed (10), from which guanidine is removed by smooth hydrolysis according to reaction (11) and formic acid decomposes to CO and  $\text{H}_2\text{O}$  according to (2).



However, in the hot exhaust gas the thermolysis of guanidinium formate to cyanamide ( $\text{H}_2\text{NCN}$ ),  $\text{NH}_3$  and formic acid might also be possible. The elucidation of the decomposition chemistry is a prerequisite for the safe application of guanidinium derivatives as SCR reducing agents and is subject of a current study in our laboratory.

For realistic investigations of the decomposition behavior of guanidinium formate and other guanidine salts, a spray injection system for aqueous solutions is required on the lab-scale. Since the downscaling of such injection systems from the real diesel engine to the laboratory apparatus is problematic, a simple droplet feeder was used in the present study and the decomposition behavior of the different guanidinium salt solutions was compared with a urea solution as reference. With this approach, qualitative statements were possible on the suitability of the new SCR reducing agents and catalytic materials could be tested. However, the preliminary character of the laboratory tests has to be emphasized.

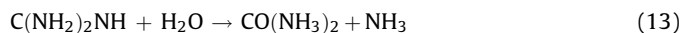
The dropwise addition of the dosing agents resulted in strong fluctuations of the measured concentrations. However, the measurement results could be evaluated by averaging over 5–10 min. It turned out during the experiments that considerable amounts of ammonia were oxidized to nitrogen in the feed, so that reference measurements without oxygen were also carried out.

**3.3.1.1. Decomposition of guanidinium formate over Fe-ZSM5.** First, a urea solution was tested as a reference reducing agent with Fe-ZSM5.  $\text{CO}_2$  was quantitatively formed and no HNCO was found, but the ammonia yield was only 92% at 300–350 °C and 3–4 ppm  $\text{N}_2\text{O}$  were formed (Table 4). However, after switching to an oxygen-free feed gas, the ammonia balance was very good and no  $\text{N}_2\text{O}$  was found. Obviously, about 8% of the ammonia was oxidized by oxygen over Fe-ZSM5 at 300 °C at such low space velocities. This ammonia oxidation is known for the SCR process, although only at higher temperatures due to the usually applied higher space velocities.

When guanidinium formate was dosed, only 25% of the guanidinium formate was decomposed to ammonia at 300 °C and 67% at 350 °C (Table 4).  $\text{CO}_2$  was found on a similar concentration level beside 185 ppm of CO, 47 ppm of formic acid and small amounts of methanamide, HCN and HNCO. At 350 °C, no significant influence of oxygen could be detected on the degree of guanidinium formate decomposition. However, the experiments at 400 and 450 °C were carried out with oxygen-free feed gas as

a measure of precaution to exclude any falsification by ammonia oxidation. With increasing temperatures, higher decomposition degrees were reached. At 400 °C, 93% of the guanidinium formate was converted and at 450 °C, 96% was converted. A reference experiment with oxygen at 450 °C showed that ammonia oxidation indeed reduced the ammonia yield from 96% to 71%.

The observed decomposition products CO, formic acid and methanamide are typical for ammonium formate or formic acid in ammonia containing gases, suggesting the decomposition of guanidinium formate to guanidine and formic acid as the first step in the decomposition process according to (10). The fact that HNCO was found in traces is an important indication of the mechanism of the guanidine hydrolysis via urea as an intermediate. Guanidine from the thermolysis of guanidinium formate probably hydrolyses to urea, which decomposes further according to the already known urea thermolysis.



**3.3.1.2. Decomposition of guanidinium formate over  $\text{TiO}_2$ .** At 300 and 350 °C, mainly ammonia,  $\text{CO}_2$  and CO were formed over  $\text{TiO}_2$  as the expected products of the guanidinium formate decomposition. Formic acid and methanamide were not observed, and less than 10 ppm of HCN were detected, which is half of the amount formed

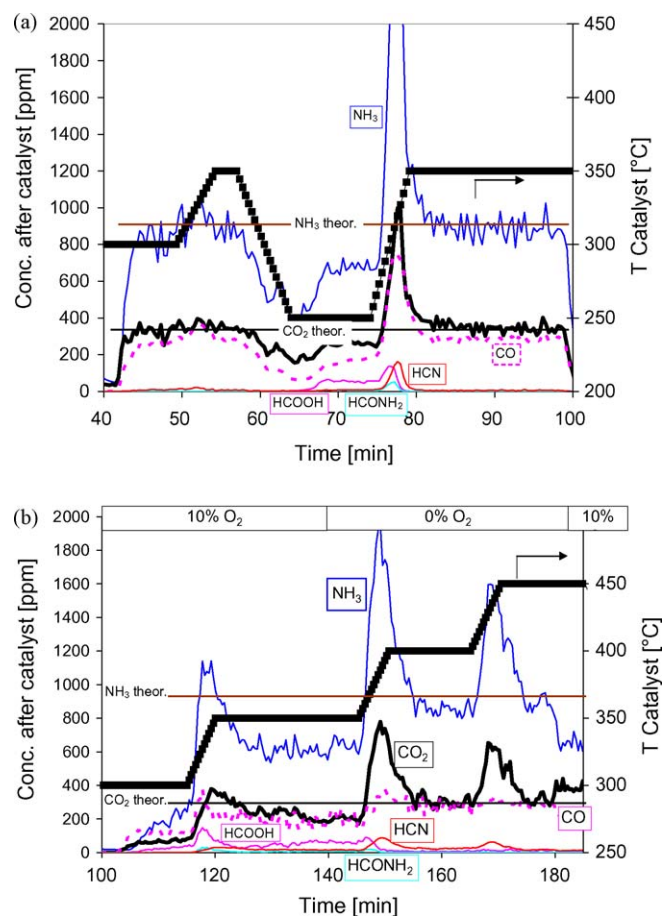


**Fig. 16.** Decomposition of guanidinium formate over (a)  $\text{TiO}_2$  and (b) Fe-ZSM5. Feed: 10%  $\text{O}_2$ , 5%  $\text{H}_2\text{O}$ , ca. 300 ppm guanidinium formate in  $\text{N}_2$ .  $T = 250$ – $350$  °C. GHSV =  $13\,000\text{ h}^{-1}$ .

over Fe-ZSM5 and only about 1% of the amount of ammonia generated. From Fig. 16a, showing the concentration profiles during guanidinium formate decomposition at different temperatures, it can be concluded that only negligible amounts of guanidinium formate or decomposition products were stored on TiO<sub>2</sub> at 300 °C, discernible from the only very small increase of the NH<sub>3</sub>, CO and CO<sub>2</sub> concentrations when the temperature rose from 300 to 350 °C at  $t = 50$ –54 min. By contrast, significant amounts of guanidinium formate were deposited on TiO<sub>2</sub> at 250 °C, confirmed by an emission peak of NH<sub>3</sub>, CO and CO<sub>2</sub> in the ratio 3:1:1 upon a temperature increase from 250 to 350 °C at  $t = 75$ –80 min.

**3.3.1.3. Decomposition of guanidinium carbonate, -hydrogen carbonate and -oxalate over TiO<sub>2</sub>.** Since formic acid is a rather strong acid ( $pK_s$  3.7), guanidinium salts of weaker acids might be easier to hydrolyze. The reaction products CO, formic acid, methanamide and HCN found in the decomposition of guanidinium formate are attributed to formate, since these products are also found with ammonium formate as the reducing agent. However, when guanidinium compounds with other anions are used, these products are no longer expected. The most important criterion for the selection of suitable salts was that the anions may be decomposed to harmless gaseous products. Moreover, the stability of the anions was varied in order to investigate the influence of this parameter on the decomposition properties. Thus, beside guanidinium formate, di-guanidinium carbonate, guanidinium hydrogen carbonate and guanidinium oxalate were selected.

With di-guanidinium carbonate, an almost 100% ammonia yield was obtained over TiO<sub>2</sub> at 300–350 °C, a 88% yield at 250 °C and a 79% yield at 225 °C (Table 5). Although the ammonia yield dropped to 30% at a catalyst temperature of 200 °C, the decomposition of guanidinium carbonate proceeded much better than that of guanidinium formate and problematic side-products were no longer detected.

Since aqueous guanidinium carbonate solution is strongly basic (pH 11–11.5), the much less basic guanidinium hydrogen carbonate was also prepared by bubbling CO<sub>2</sub> through a di-guanidinium carbonate solution. The required amounts of CO<sub>2</sub> were about 4–5 times higher than theoretically expected due to the relatively slow dissolution of CO<sub>2</sub> in water, so that the major part of the CO<sub>2</sub> remains in the gas phase after the short contact time in the liquid. During the preparation, after a first quick descent of the pH value by ca. 1, a continuous decline was observed, running out to a constant pH value of 8.4. Fig. 17 shows the equilibria between CO<sub>2</sub>, hydrogen carbonate and carbonate in dependency of the pH value, as they are expected, when feeding CO<sub>2</sub> into a guanidinium

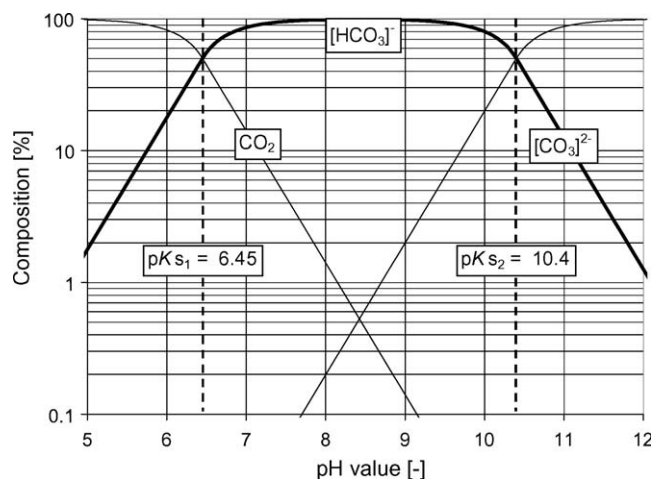


Fig. 17. Equilibrium between CO<sub>2</sub>, hydrogen carbonate and carbonate in dependency of the pH value.

carbonate solution. Pure di-guanidinium carbonate solution has a very high pH value of around 11.5, at which 95% is present as carbonate and 5% as hydrogen carbonate. For solutions with 50% di-guanidinium carbonate and hydrogen carbonate each, a pH value of 10.5 is expected according to Fig. 17. Moderate pH values of around 9 may only be realized with pure guanidinium hydrogen carbonate solutions, and still lower pH values are not feasible without the degassing of CO<sub>2</sub>. In our experiments, a constant pH value of 8.4 was reached, at which CO<sub>2</sub> uptake and release of the solution was in equilibrium.

Similar ammonia yields were obtained with guanidinium hydrogen carbonate compared to the carbonate between 250 and 350 °C, and the values were even slightly higher at 225 and 250 °C (Table 5). No additional side-products were observed, as expected.

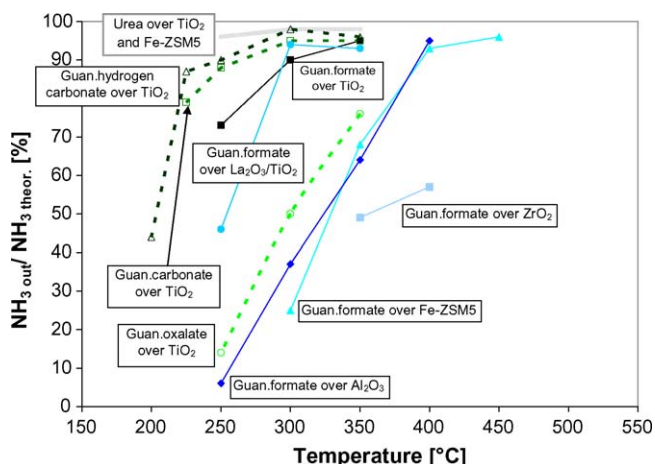
The catalytic hydrolysis of guanidinium oxalate proved to be very difficult. At 350 °C the ammonia yield was 76%, and at 300 °C, it decreased to 50%. CO was formed by thermolysis of the oxalate and a few ppm of HCN was observed (Table 4). After dismounting the coated catalyst, the frontal area showed black deposits, pointing to an incomplete decomposition of the guanidinium oxalate.

Fig. 18 summarizes the measured ammonia yields of the decomposition experiments with the different guanidinium salts over TiO<sub>2</sub>. The decomposition behaviour of the different guanidi-

Table 5

Thermohydrolysis of di-guanidinium carbonate (15%) and guanidinium hydrogen carbonate (19.5%) on TiO<sub>2</sub> and Fe-ZSM5 coated on cordierite monoliths (400 cps). Dosage of the reducing agent by dropping on the catalyst entrance. GHSV = 13 000 h<sup>-1</sup>. Basis feed gas: 5% H<sub>2</sub>O in N<sub>2</sub>. The concentrations of HNCO, CO, HCOOH, methanamide and HCN were below 1 ppm except for (1) and (2).

$T_{cat}$ [°C]	Ammonia precursor compound	Catalyst	O <sub>2</sub> [%]	Y <sub>CO<sub>2</sub></sub> [%]	Y <sub>NH<sub>3</sub></sub> [%]
200	di-Guanidinium carbonate (15%)	TiO <sub>2</sub>	10	36	30
225	di-Guanidinium carbonate (15%)	TiO <sub>2</sub>	10	82	79
250	di-Guanidinium carbonate (15%)	TiO <sub>2</sub>	10	91	88
300	di-Guanidinium carbonate (15%)	TiO <sub>2</sub>	10	100	96
350	di-Guanidinium carbonate (15%)	TiO <sub>2</sub>	10	100	95
200	Guanidinium hydrogen carbonate (19.5%)	TiO <sub>2</sub>	10	62	44
225	Guanidinium hydrogen carbonate (19.5%)	TiO <sub>2</sub>	10	90	87
250	Guanidinium hydrogen carbonate (19.5%)	TiO <sub>2</sub>	10	95	90
300	Guanidinium hydrogen carbonate (19.5%)	TiO <sub>2</sub>	10	100	98
350	Guanidinium hydrogen carbonate (19.5%)	TiO <sub>2</sub>	10	99	96
250	di-Guanidinium carbonate (15%)	Fe-ZSM5	0	50	37
300	di-Guanidinium carbonate (15%)	Fe-ZSM5	0	60	58
350	di-Guanidinium carbonate (15%)	Fe-ZSM5	0	88	87
400	di-Guanidinium carbonate (15%)	Fe-ZSM5	0	100	97 <sup>(1)</sup>
450	di-Guanidinium carbonate (15%)	Fe-ZSM5	0	100	99 <sup>(2)</sup>



**Fig. 18.** Overview of the ammonia yields in the laboratory experiments on the decomposition of guanidinium formate over different catalysts and of different guanidinium salts over  $\text{TiO}_2$ . Feed: ca. 300 ppm guanidinium salt, 5%  $\text{H}_2\text{O}$  in  $\text{N}_2$ .  $T = 250\text{--}350^\circ\text{C}$ . GHSV =  $13\,000\text{ h}^{-1}$ .

nium salts is correlated with the basicity of the anions: the weaker the basicity (i.e., the stronger the corresponding acids), the more difficult the thermal dissociation of these salts is, which precedes the decomposition on the catalyst. In accordance with this correlation, the  $\text{pKs}$  for the first protolysis of oxalic acid has a value of 1.2, which is much lower than that of formic acid ( $\text{pKs} = 3.7$ ).

Regarding the reaction temperature and selectivity of the decomposition reaction, guanidinium carbonate and hydrogen carbonate appeared as promising alternatives to guanidinium formate. However, the better decomposition properties were connected with a lower stability of these guanidinium derivatives in aqueous solution, which is critical under consideration of the practical application. Moreover, a markedly lower solubility in water was found for the two carbonates. The catalytic tests revealed another critical feature of the guanidinium carbonate salts: the  $\text{TiO}_2$  coating of the monoliths showed a poor stability. The first catalytic module lost 80% of the active mass and for the whole catalytic converter, the loss summed up to 50% of the catalytic coating. The flaking off of the catalyst should have no significant influence on the measuring results, as the catalytic material stayed in the reactor and was still available for the hydrolysis. A test of the coating quality with water in an ultrasonic bath showed that the adhesive strength was sufficient. Although about 15% of the coating peeled off during the first 5 min of treatment in the ultrasonic bath, only traces were lost thereafter. The observed loss of the  $\text{TiO}_2$  coating is remarkable, since the same amount of colloid ammonium silicate was used as an inorganic binder as for the preparation of  $\text{V}_2\text{O}_5/\text{WO}_3\text{-TiO}_2$  SCR catalysts according to [28], which proved its good abrasion resistance in urea SCR in Diesel test rig experiments. The reason for the erosion of the  $\text{TiO}_2$  coating is therefore more likely found in the dissolution of the silica binder by the strongly basic reducing agents, and this should be checked with commercial hydrolysis catalysts.

**3.3.1.4. Decomposition of guanidinium derivatives over Fe-ZSM5 and other catalysts.** The concentration profiles during the guanidinium formate decomposition on Fe-ZSM5 were measured in dependency of the temperature (Fig. 16b) and compared to the corresponding profiles for  $\text{TiO}_2$  (Fig. 16a). In contrast to  $\text{TiO}_2$ , guanidinium formate was not quantitatively decomposed over Fe-ZSM5 at  $300^\circ\text{C}$  and various decomposition products were stored on the catalyst, which desorbed during the temperature ramp from 300 to  $350^\circ\text{C}$  at

$t = 115\text{--}120\text{ min}$ . Please note that oxygen was switched off at  $350^\circ\text{C}$ , since  $\text{NH}_3$  started to be oxidized to nitrogen at the applied low GHSV of  $13\,000\text{ h}^{-1}$ . During the temperature ramps from 350 to 400 and from 400 to  $450^\circ\text{C}$ , huge amounts of  $\text{NH}_3$  and  $\text{CO}_2$  were generated in a ratio of 3:1, whereas an increase of the  $\text{CO}$  emissions was not observed. Since formate would have been decomposed to  $\text{CO}$  upon a temperature increase, guanidinium was not adsorbed as its formate on the catalyst surface. It is rather likely that guanidinium was adsorbed as a stable cation at the strong Brønsted acid sites of Fe-ZSM5. The high acidity of Fe-ZSM5 and the connected stabilization of guanidinium as a cation is probably the main reason for the bad decomposition properties of this catalyst. Such a stabilization of guanidinium as a cation is missing on amphoteric  $\text{TiO}_2$ , on which the free guanidine base is hydrolyzed to ammonia and urea.

Aside from the strong Brønsted acidity, the stabilization on Fe-ZSM5 could also be caused by the formic acid. It was tested with guanidinium carbonate whether Fe-ZSM5 is a bad hydrolysis catalyst for guanidine in general due to the high surface acidity or if the stabilization of guanidine is also determined by the anion, giving rise to the assumption that guanidinium carbonate might be more decomposable. The experiments were carried out without oxygen since ammonia is partly oxidized over Fe-ZSM5 above  $350^\circ\text{C}$ . Over Fe-ZSM5, guanidinium carbonate is completely hydrolyzed at  $400\text{--}450^\circ\text{C}$  (Table 5). At  $350^\circ\text{C}$ , the ammonia yield decreases and reaches only 60% at  $300^\circ\text{C}$ . At 400 and  $450^\circ\text{C}$ , a few ppm of  $\text{HNCO}$  and traces of  $\text{HCN}$  were found beside ammonia and  $\text{CO}_2$ . Though the hydrolysis of guanidinium carbonate proceeds better than that of guanidinium formate, it is still insufficient for a practical application.

In summary, it can be stated that the guanidinium cation is stabilized on the strongly acidic Fe-ZSM5, thereby aggravating its decomposition. But the acidity of the anions also has significant influence on the stabilization of guanidinium. Guanidinium formate is generally more difficult to hydrolyze than guanidinium carbonate or the hydrogen carbonate.

The hydrolysis of guanidinium formate over  $\gamma\text{-Al}_2\text{O}_3$  proceeded much worse than expected from the excellent properties of this material for urea decomposition. Quantitative conversion was reached at  $400^\circ\text{C}$ , but at lower temperatures, the ammonia yield dropped. The values were similar to those for Fe-ZSM5, but without the pronounced ammonia oxidation, which was observed for that catalyst. The difference in activity of  $\gamma\text{-Al}_2\text{O}_3$  for urea and guanidinium formate decomposition indicates that both compounds follow different decomposition pathways, which prevents a simple transfer of the catalyst technology from the urea thermohydrolysis reaction to the new guanidinium salts. Guanidinium oxalate was hydrolyzed as bad as the formate over  $\text{Al}_2\text{O}_3$ .

Over lanthanum oxide doped  $\text{TiO}_2$  ( $\text{La}_2\text{O}_3/\text{TiO}_2$ ), guanidinium formate was hydrolyzed at 300 and  $350^\circ\text{C}$  with a high ammonia yield. However, at  $250^\circ\text{C}$  the ammonia yield was only 46%, which is significantly lower than for pure  $\text{TiO}_2$ . The basic lanthanum oxide also did not positively influence the hydrolysis of guanidinium oxalate.

Guanidinium formate was also badly converted on weakly basic zirconia ( $\text{ZrO}_2$ ). Even at  $400^\circ\text{C}$ , the ammonia yield was only about 60% and the high slip of formic acid was remarkable, only half of it decomposing to  $\text{CO}$ . From the tested catalyst materials, the following order of activities can be deduced for the hydrolysis of guanidinium compounds, which is headed by  $\text{TiO}_2$ :  $\text{TiO}_2 > \text{La}_2\text{O}_3/\text{TiO}_2 \gg \gamma\text{-Al}_2\text{O}_3 > \text{Fe-ZSM5} > \text{ZrO}_2$  (Fig. 18).

**3.3.1.5. Optimization of reaction conditions for the decomposition of guanidinium formate over  $\text{TiO}_2$ .** On the basis of the promising results of the guanidinium formate decomposition over  $\text{TiO}_2$  in the



anatase modification, we tried to optimize the reaction temperature and the space velocity for total conversion. By addition of a TiO<sub>2</sub> pellet bed downstream of the coated monoliths, and by reduction of the flow rate from 0.45 to 0.40 m<sup>3</sup>/h, the GHSV was reduced by a factor of 3.5 from 13 000 to 3800 h<sup>-1</sup>. In fact, guanidinium formate could be easily decomposed at 300–400 °C at such low space velocities. Only ammonia, CO and CO<sub>2</sub> were found in the expected ratio according to (12), and no side-products were formed. The emission peaks of ammonia in the heating phases from 300 to 350 and from 350 to 400 °C were caused by the large amount of TiO<sub>2</sub> catalyst present in the reactor, from which the ammonia desorbed due to the lower storage capacity of the catalyst at higher temperatures.

The laboratory experiments were of only limited significance mainly due to the application of liquid SCR reducing agents, which had to be evaporated. The dropwise addition of the guanidinium formate solution on a small area with a diameter of 8–10 mm resulted in a bad exploitation of the catalyst. Moreover, the catalyst structure allowed for only small heat flow in the radial direction, i.e., the heat for the evaporation of the water and the thermolysis was primarily provided by the gas phase.

**3.3.1.6. Remarks on HCN emissions.** The small HCN emissions found in part of the laboratory experiments varied with the type of guanidinium salt, the decomposition catalyst and the reaction conditions. This might be rationalized by a suppression of HCN formation over specific catalytic materials or by an oxidation or hydrolysis of intermediately formed HCN over suitable decomposition catalysts. The second explanation prompted us to investigate the possibility of oxidizing or hydrolyzing HCN over different catalytic materials. It appeared from these experiments, for which details will be described in another publication, that HCN in fact may be efficiently oxidized and hydrolyzed over certain decomposition and SCR catalysts [35]. For instance, HCN was hydrolyzed over TiO<sub>2</sub> and H-ZSM5 to ammonia and CO, it was hydrolyzed and oxidized over Fe-ZSM5, and it was mainly oxidized over Cu-ZSM5 to N<sub>2</sub>, NO and CO<sub>2</sub> [35]. These results are very important in view of a practical application of guanidinium salts as ammonia precursor compounds, because they prove on one side that a generously dimensioned TiO<sub>2</sub> catalyst is able to quantitatively decompose HCN beside its proven suitability for the decomposition of guanidinium salts, and on the other side, that even in the case of HCN emissions, they may be converted over a downstream zeolite-based SCR catalyst. Another possibility to completely avoid HCN emissions is the application of a precious metal-based oxidation catalyst downstream of the SCR catalyst, which oxidizes not only the ammonia slip but also HCN [36]. Although HCN emissions are not expected in the practical application on the basis of these results, it should be mentioned that HCN emissions are well known in automotive catalysis and that only recently three-way catalysts have become available that do not show HCN emissions [37].

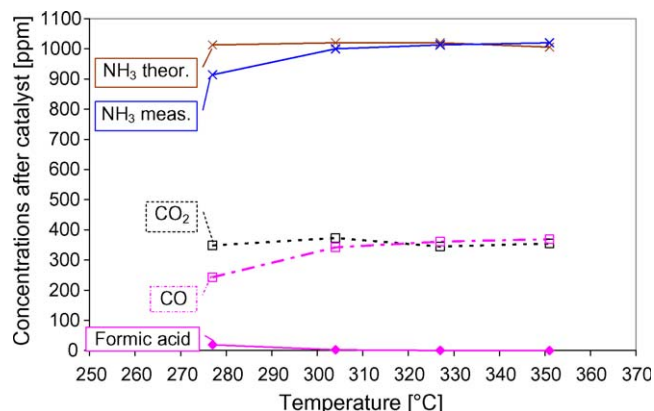


**Fig. 19.** Decomposition of an aqueous guanidinium formate solution (60%) over TiO<sub>2</sub> in the pilot plant. Reducing agent: 282 ± 2 g/h. Basis feed: 5% H<sub>2</sub>O in 100 m<sup>3</sup>/h air. GHSV = 30 000 h<sup>-1</sup>.

### 3.3.2. Decomposition of guanidinium formate over TiO<sub>2</sub> in the pilot plant

In order to narrow down the temperature ranges and space velocities for the decomposition of guanidinium formate under realistic conditions, pilot plant experiments were carried out for continuative investigations with a 60% guanidinium formate solution (Fig. 19).

A 32.5% urea solution (AdBlue<sup>®</sup>) was tested first in the pilot plant as a reference, which was virtually quantitatively decomposed to NH<sub>3</sub> and CO<sub>2</sub> in the tested temperature range from 275 to 350 °C (Table 6). With the guanidinium formate solution, total conversion was also reached between 300 and 350 °C (Fig. 18; Table 6), which is in contrast to the results in the laboratory, where much lower conversions were observed. This is a clear indication of the importance of a proper reaction design and especially of a spray injection to facilitate full conversion of guanidinium formate at high selectivity. Only negligible amounts of HNCO and HCN were formed over the entire temperature range.

At 275 °C, the ammonia yield slightly decreased to 91%, whereas CO<sub>2</sub> was formed in the expected amounts, according to the stoichiometry of the decomposition reactions, but the CO concentration was only 72% of the theoretical level. That means that the hydrolysis of guanidinium was complete, yielding CO<sub>2</sub>, and that formic acid was only partially decomposed to CO. From the lack of CO and NH<sub>3</sub>, it can be deduced that ammonium formate or methanamide was deposited on the catalyst, which is not surprising under consideration of the large amount of TiO<sub>2</sub> available for adsorption.

In all experiments with the injection of guanidinium formate solution, a colorless condensation film was found at the inner wall of the quartz tube upstream of the catalyst, and it was more pronounced at low temperatures. It has to be pointed out that the

**Table 6**

Results of the pilot plant experiments with guanidinium formate solution (60%) over TiO<sub>2</sub>. Reducing agent: 282 ± 2 g/h. Basis feed: 100 m<sup>3</sup>/h air, 5% H<sub>2</sub>O. GHSV = 30 000 h<sup>-1</sup>.

T <sub>cat</sub> [°C]	Ammonia precursor compound	Reducing agent [g/h]	Y <sub>CO<sub>2</sub></sub> [%]	Y <sub>NH<sub>3</sub></sub> [%]	HNCO [ppm]	CO [ppm]	HCOOH [ppm]	Methanamide [ppm]	HCN [ppm]
275	Urea solution (32.5%)	417	103	99	1	0	0	0	0
300	Urea solution (32.5%)	420	104	100	2	0	0	0	0
325	Urea solution (32.5%)	421	103	99	1	0	0	0	0
350	Urea solution (32.5%)	418	103	101	1	0	0	0	0
275	Guanidinium formate solution (60%)	282	103	91	1	72	16	3	3
300	Guanidinium formate solution (60%)	284	108	98	1	101	2	0	6
325	Guanidinium formate solution (60%)	284	101	99	1	106	0	0	6
350	Guanidinium formate solution (60%)	280	106	102	1	110	0	0	6

film formation was completely reversible and that solid deposits were not formed. The film, which was likely composed of guanidine or molten guanidinium formate, evaporated completely within 1–2 min after dosage stop or when switching to the injection of water or urea solution. This behavior of guanidinium formate solution differs from that of urea solution, which tends to form cyanuric acid or other side-products when sprayed on relatively cold surfaces. One may speculate that the reason for the observed reversible film formation is a combination of larger spray droplets, which are harder to evaporate, with the different chemical properties of guanidinium formate, which does not tend to form hardly thermolizable deposits.

When the experiments were carried out without water in the feed gas, it turned out that the decomposition proceeded worse and that HNCO, formic acid, HCN and methanamide were formed aside from the expected main reaction products  $\text{NH}_3$ , CO and  $\text{CO}_2$ . This behavior is plausible in view of the proposed reaction mechanism with its multiple reaction steps. The laboratory tests revealed that the most difficult part of the guanidinium formate decomposition is the hydrolysis of guanidine, from which the first and the third reaction step, namely the hydrolysis of guanidine to urea and the hydrolysis of HNCO to ammonia, require water as reactant. One may easily imagine that HNCO is emitted from the reactor with a water deficiency in this last hydrolysis reaction. Moreover, we know from the ammonium formate experiments that methanamide is easily formed from ammonia and formic acid, and both are produced in the course of guanidinium formate decomposition. Since methanamide also needs water to be hydrolyzed, it was emitted when the water dosing was switched off. Finally, HCN was formed from methanamide by dehydration according to (6) – a reaction with a negative free enthalpy at high temperatures. Moreover, in the absence of water in the feed, this reaction is shifted to the product side. Other measures to improve the guanidinium formate decomposition were much less effective than the addition of water to the feed. Reducing the dosage of the guanidinium formate solution increased the  $\text{NH}_3$  yield, but the concentration of the side-products remained at an inadmissible level. By raising the temperature, the  $\text{NH}_3$  yield could in fact be increased and the side-products HNCO and formic acid reduced, but in return, the CO and HCN concentrations increased significantly. The water content in 60% guanidinium formate solution is 3.9 times more than the amount of water that is theoretically required for the quantitative decomposition of guanidinium formate according to (12). However, the pilot plant experiments without water clearly showed that the reaction needs water in high excess to shift the equilibrium of the reactions in the direction of the desired products ammonia, CO and  $\text{CO}_2$ . As exhaust gases from combustion processes contain high levels of water anyway, this advantageous condition is always met in SCR systems.

#### 4. Conclusions

It was shown by means of model gas investigations that ammonium formate may be applied as an ammonia precursor compound in the SCR reaction over both  $\text{V}_2\text{O}_5/\text{WO}_3\text{-TiO}_2$  and Fe-ZSM5 catalysts. However, formic acid was emitted at low temperatures in considerable amounts, which may cause corrosion problems when applied in real SCR systems. It was observed that the formic acid present at low temperatures also reacts with ammonia in an amidation reaction to furnish large amounts of methanamide, especially when ammonia was overdosed. At higher temperatures, formic acid decomposed quantitatively to water and CO, which may be oxidized in a real exhaust gas system over a small oxidation catalyst. A significant reduction of the  $\text{NO}_x$

reduction efficiencies has to be accepted over  $\text{V}_2\text{O}_5/\text{WO}_3\text{-TiO}_2$ , and even more pronounced over Fe-ZSM5 in the low temperature regime under  $\text{NO}/\text{NO}_2$  SCR conditions, because  $\text{NO}_2$  reacts with formic acid to form  $\text{CO}_2$  and NO, which has a lower SCR activity. It could be shown that the stronger deactivation over Fe-ZSM5 is also caused by the deposition of large amounts of ammonium formate and ammonium nitrate in the pores of the zeolite. These deposits could be removed by heating the Fe-ZSM5 catalyst, but HCN was also formed, which is problematic in light of very similar transient conditions in real SCR systems.

Methanamide cannot be applied as a direct substitute for urea solution, which is injected into the exhaust gas in the SCR process, because it was not completely decomposed at low temperatures and produced significant amounts of HCN at higher temperatures over typical SCR catalysts. However, methanamide proved to be quantitatively decomposable to  $\text{NH}_3$  and CO over  $\text{TiO}_2$  at 300–350 °C, which renders the application of methanamide in the SCR process possible – not as a direct SCR reducing agent, but as an ammonia precursor compound, which may be decomposed in an external ammonia generator.

Guanidinium salts, and especially guanidinium formate, are promising new ammonia precursor compounds for utilization in the SCR process. Unlike urea or ammonium formate solutions, guanidinium formate solution is very stable even when continuously heated to 100 °C. However, this high stability has the consequence that guanidinium formate is also not quantitatively decomposable at 200 °C, which is the required starting temperature for SCR. The results of our study showed that – similar to methanamide –  $\text{TiO}_2$  was the best decomposition catalyst for guanidinium compounds. In combination with the required decomposition temperature of 300 °C and a moderate space velocity of  $30\,000\text{ h}^{-1}$ , a separate ammonia generator would also be the best solution for the application of this ammonia precursor compound in the SCR process. All experimental results were in agreement with the formation of ammonia from guanidinium formate in three reaction steps: (1) decomposition of guanidinium formate to the free guanidine base and formic acid, (2) hydrolysis of guanidine to ammonia and carbon dioxide via urea and HNCO as intermediates and (3) decomposition of formic acid to water and CO.

#### Acknowledgements

We are indebted to Th. Sattelmayer for the use of the pilot plant at the TU Munich and thank S. Steinbach and U. Glöckert for their valuable support. We are much obliged to AlzChem Trostberg GmbH and Nigu Chemie GmbH for funding the experiments with the guanidinium derivatives in the framework of a research contract.

#### References

- [1] H. Bosch, F. Janssen, *Catal. Today* 2 (1988) 369.
- [2] M. Wojciechowska, S. Lomnicki, *Clean Products Process.* 1 (1999) 237.
- [3] M.V. Twigg, *Appl. Catal. B* 70 (2007) 2.
- [4] F.A. Perry, D.L. Siebers, *Nature* 324 (1986) 657.
- [5] M. Koebel, M. Elsener, T. Marti, *Combust. Sci. Technol.* 121 (1996) 85.
- [6] B. Maurer, E. Jacob, W. Weisweiler, *MTZ Worldwide* 60 (1999) 12.
- [7] B. Elvers, 5th ed., *Ullmann's Encyclopedia of Industrial Chemistry*, vol. A27, VCH, Weinheim, 1996, pp. 358–365.
- [8] W.-P. Trautwein, *AdBlue as a Reducing Agent for the Decrease of  $\text{NO}_x$  Emissions from Diesel Engines of Commercial Vehicles*, Part 1 + 2, German Society for Petroleum and Coal Science and Technology, DGMK-Research Report 616-1, Hamburg, 2003, DGMK-Research Report 616-2, Hamburg, 2005.
- [9] P.M. Schaber, J. Colson, S. Higgins, D. Thielen, B. Anspach, J. Brauer, *Thermochim. Acta* 424 (2004) 131.
- [10] P. Tennison, Ch. Lambert, M. Levin, *SAE Trans.*, J. Fuels Lubricants 113 (2004) 573.
- [11] O. Kröcher, M. Elsener, E. Jacob, in: *Proceedings of the 5th International Exhaust Gas and Particulate Emissions Forum*, 19–20 February 2008, Ludwigsburg, Ger-

- many, (2008), pp. 98–119. Download: [http://ega.web.psi.ch/Krocher\\_Emission\\_Forum\\_2008.pdf](http://ega.web.psi.ch/Krocher_Emission_Forum_2008.pdf).
- [12] Ch. Bernhart, *Swiss Eng.* 9 (2006) 35.
- [13] W. Kind, E. Jacob, W. Müller, *MTZ Worldwide* 62 (2001) 70.
- [14] W. Weisweiler, F. Buchholz, *Chem. Ing. Tech.* 73 (2001) 882.
- [15] W. Müller, A. Herr, S. Käfer, A. Lacroix, E. Jacob, SCR Using Solid Urea, *Proceedings of the 3rd International Exhaust Gas and Particulate Emissions Forum*, 14–15 September 2004, Sinsheim, Germany, (2004), pp. 230–242.
- [16] H.-O. Herrmann, M.M. Hernier, V. Scholz, in: H.P. Lenz (Ed.), *A Solid SCR System for Diesel Passenger Cars and Light-Duty Trucks*, 23rd Vienna International Motor Symposium, 25–26 April 2002, Vienna, Austria, VDI-Fortschrittberichte, Series No. 12, vol. 490/2, pp. 217–233.
- [17] M. Krüger, P. Nisius, V. Scholz, A. Wiartalla, *MTZ Worldwide* 6 (2003).
- [18] A. Solla, M. Westerholm, Ch. Söderström, K. Tormonen, T. Härmä, T. Nissinen, J. Kukkonen, *SAE Technical Paper Series* 2005-01-1856.
- [19] M. Koebel, M. Elsener, *Ind. Eng. Chem. Res.* 37 (1998) 3864.
- [20] T.D. Elmøe, R.Z. Sørensen, U. Quaade, C.H. Christensen, J.K. Nørskov, T. Johannesssen, *Chem. Eng. Sci.* 61 (2006) 2618.
- [21] E. Jacob, Perspectives on Mobile SCR Technology, *Proceedings of the 15th Aachen Colloquium "Automobile and Engine Technology"*, 9–11 October 2006, Aachen, Germany, vol. 2, 2006, pp. 1303–1336. Download: [http://www.emitec.com/download/library/en/061030\\_Aachen\\_SCR\\_engl\\_final.pdf](http://www.emitec.com/download/library/en/061030_Aachen_SCR_engl_final.pdf).
- [22] P.L.T. Gabrielsson, *Top. Catal.* 28 (2004) 177.
- [23] C. Grambow, S. Weiss, R. Youngman, B. Antelmann, B. Mertschenk, K.P. Stengele, 6th ed., *Ullmann's Encyclopedia of Industrial Chemistry*, vol. 16, Wiley-VCH, Weinheim, Germany, 2003, pp. 73–86.
- [24] O. Kröcher, M. Elsener, U. Glückert, Th. Sattelmayer, E. Jacob, B. Hammer, H.-P. Krimmer, in: *Proceedings of the 2nd Conference MinNO<sub>x</sub>—Minimization of NO<sub>x</sub> Emissions Through Exhaust Aftertreatment*, Berlin, 19–20 June 2008, Haus der Technik, Essen, 2008.
- [25] Data Sheets from Alzchem Trostberg, 2008.
- [26] M. Koebel, E.O. Strutz, *Ind. Eng. Chem. Res.* 42 (2003) 2093.
- [27] M. Devadas, O. Kröcher, A. Wokaun, *React. Kinet. Catal. Lett.* 86 (2005) 347.
- [28] O. Kröcher, *Stud. Surf. Sci. Catal.* 171 (2007) 261.
- [29] M. Koebel, M. Elsener, G. Madia, *SAE Technical Paper Series* 2001-01-3625.
- [30] S. Steinbach, Einfluss der Transportvorgänge auf die Effizienz von Harnstoffkatalysatoren in SCR-Abgasanlagen, Ph.D. thesis, TU Munich, Germany, Verlag Dr. Hut, 2007, ISBN 978-3-89963-576-8, Download: <http://www.td.mw.tum.de/tum-td/de/forschung/dissertationen/download/C2007/steinbach.pdf>.
- [31] N. Akiya, Ph.E. Savage, *AIChE J.* 44 (1998) 405.
- [32] M. Koebel, M. Elsener, O. Kröcher, Ch. Schär, R. Röthlisberger, F. Jaussi, M. Mangold, *Top. Catal.* 30/31 (2004) 43.
- [33] C. Ciardelli, I. Nova, E. Tronconi, B. Konrad, D. Chatterjee, K. Ecke, M. Weibel, *Chem. Eng. Sci.* 59 (2004) 5301.
- [34] O. Kröcher, M. Devadas, M. Elsener, A. Wokaun, N. Söger, M. Pfeifer, Y. Demel, L. Musmann, *Appl. Catal. B* 66 (2006) 208.
- [35] O. Kröcher, M. Elsener, Katalytische Hydrolyse und Oxidation von HCN, Report No. TM-5304-08-01, Paul Scherrer Institute, 2008.
- [36] H. Zhao, R.G. Tonkyn, S.E. Barlow, B.E. Koel, Ch.H.F. Peden, *Appl. Catal. B* 65 (2006) 282.
- [37] H.L. Karlsson, *Sci. Total Environ.* 334–335 (2004) 125.